

UNCLASSIFIED

REPORT DOCUMENTATION PAGE

AD-A211 744

TIC
 ECTE
 DATE
 3111989
 CS D

1b. RESTRICTIVE MARKINGS **THE FILE COPY**
 3 DISTRIBUTION/AVAILABILITY OF REPORT
 Approved for Public Release;
 Distribution Unlimited (2)

4 PERFORMING ORGANIZATION REPORT NUMBER(S)
 PSU-ME-R-88/89-0068

5 MONITORING ORGANIZATION REPORT NUMBER(S)
AFOUR-TR. 89-1055

6a NAME OF PERFORMING ORGANIZATION
 Dept. of Mechanical Engineering
 Penn State University

6b OFFICE SYMBOL
 (If applicable)

7a NAME OF MONITORING ORGANIZATION
 Air Force Office of Scientific Research

6c ADDRESS (City, State, and ZIP Code)
 University Park, PA 16802

7b ADDRESS (City, State, and ZIP Code)
 Building 410, Bolling AFB
 Washington, DC 20332

8a NAME OF FUNDING/SPONSORING ORGANIZATION
 Air Force Office of Sci. Res.

8b OFFICE SYMBOL
 (If applicable)
 AFOSR/NA

9 PROCUREMENT INSTRUMENT IDENTIFICATION NUMBER
 AFOSR-86-0082

8c ADDRESS (City, State, and ZIP Code)
 Building 410, Bolling AFB
 Washington, DC 20332

10. SOURCE OF FUNDING NUMBERS

PROGRAM ELEMENT NO.	PROJECT NO.	TASK NO.	WORK UNIT ACCESSION NO.
6902	2307	A1	

11. TITLE (Include Security Classification)
 Experimental Research on Swept Shock Wave/Boundary Layer Interactions

12 PERSONAL AUTHOR(S)
 Gary S. Settles

13a TYPE OF REPORT
 Final TR

13b. TIME COVERED
 FROM 86/4/1 TO 89/3/31

14. DATE OF REPORT (Year, Month, Day)
 89/6/28

15. PAGE COUNT
 39

16. SUPPLEMENTARY NOTATION

17. COSATI CODES

FIELD	GROUP	SUB-GROUP
7502		
7535		

18. SUBJECT TERMS (Continue on reverse if necessary and identify by block number)
 Shock Wave Interactions, Interactional Aerodynamics, Compressible Boundary Layers, Turbulent Boundary Layers, Supersonic Wind Tunnels, Flow Visualization, Optical Measuring Instruments, Skin Friction, Flow Distribution

19 ABSTRACT (Continue on reverse if necessary and identify by block number)
 An experimental research effort of the Penn State Gas Dynamics Laboratory on the subject of swept shock wave interactions with turbulent boundary layers is reported. This three-year study was supported by AFOSR Grant 86-0082. The research relied largely on non-intrusive, laser-based optical flow diagnostics. Experiments were carried out to define the Mach number influence, flowfield structure, and quantitative skin friction behavior of fin-generated swept interactions over the supersonic range from Mach 2.5 to 4.0, including weak, moderate, and strong interactions. The results of this research have given new insight into the fin-interaction flowfield structure, which involves a jet-impingement process caused by shock-wave bifurcation. High skin friction levels were measured in the vicinity of this jet impingement and were used for the validation of computational predictions carried out by others.

20. DISTRIBUTION/AVAILABILITY OF ABSTRACT
 UNCLASSIFIED/UNLIMITED SAME AS RPT. DTIC USERS

21. ABSTRACT SECURITY CLASSIFICATION
 Unclassified

22a. NAME OF RESPONSIBLE INDIVIDUAL
 LEONIDAS SAKELL

22b. TELEPHONE (Include Area Code)
 202-767-4935

22c. OFFICE SYMBOL
 AFOSR/NA

AFOUR-IR-89-1050

**Department of Mechanical Engineering
Pennsylvania State University
University Park, PA 16802**

Report PSU-ME-R-88/89-0068

Experimental Research on Swept Shock Wave/Boundary Layer Interactions

by Prof. Gary S. Settles

**Final Technical Report for the Period 1 April 1986
to 31 March 1989 on Grant AFOSR-86-0082**

submitted to:

**Dr. Leonidas Sakell, Program Manager
US Air Force Office of Scientific Research
Bldg. 410, Bolling AFB, DC 20332-6448**

June 1989

PENNSSTATE

Gas Dynamics Laboratory



Table of Contents

I. Summary	1
II. Introduction	1
III. Research Accomplishments	1
1) Facility Effects	1
2) Mach Number Effects	3
3) Optical Flowfield Structure Results	5
Pulsed-Laser Holographic Interferometry Results	5
Laser-Light-Screen Results	10
Conical White-Light Shadowgraphy Results	10
4) Laser Interferometer Skin Friction Results	10
IV. Conclusions and Recommendations for Future Work	12
V. Publications	14
VI. References	15
VII. Figures	17

Accession For	
NTIS CRA&I	<input checked="" type="checkbox"/>
DTIC TAB	<input type="checkbox"/>
Unannounced	<input type="checkbox"/>
Justification	
By	
Distribution/	
Availability Codes	
Dist	Availability Codes
A-1	



I. Summary

An experimental research effort of the Penn State Gas Dynamics Laboratory on the subject of swept shock wave interactions with turbulent boundary layers is reported. This three-year study was supported by AFOSR Grant 86-0082. The research relied largely on non-intrusive, laser-based optical flow diagnostics. Experiments were carried out to define the Mach number influence, flowfield structure, and quantitative skin friction behavior of fin-generated swept interactions over the supersonic range from Mach 2.5 to 4.0, including weak, moderate, and strong interactions. The results of this research have given new insight into the fin-interaction flowfield structure, which involves a jet-impingement process caused by shock-wave bifurcation. High skin friction levels were measured in the vicinity of this jet impingement and were used for the validation of computational predictions carried out by others.

II. Introduction

The swept interactions of shock waves with turbulent boundary layers constitute one of the fundamental problems of modern gas dynamics. These strong viscous/inviscid interactions are extremely difficult to understand theoretically or to predict by computational methods. Nonetheless, they are of critical importance in the aerodynamic performance of current and future flight vehicles, both military and commercial. For these reasons, swept interactions have become a major test case for the validation of advanced Computational Fluid Dynamics (CFD) codes.

The review by Settles and Dolling¹ covers the progress of research on this problem up to 1986. Among many questions raised in this research, the influence of variable Mach number and shock strength, the structure of the flowfield, and the physical mechanisms responsible for its behavior remained poorly understood at the time. The need for an improved scientific understanding of these issues and the demand for high-quality experimental data to validate CFD methods has led to several recent studies of swept interactions, both in the US and abroad.

This Final Technical Report on AFOSR Grant 86-0082 summarizes research carried out at the Gas Dynamics Laboratory of Penn State University on swept shock wave/turbulent boundary layer interactions over the period 1 April 1986 to 31 March 1989. Detailed results and data from this experimental research effort have been presented at international symposia and submitted for archival journal publication, as indicated in section V. of this Report.

III. Research Accomplishments

1) Facility Effects

An important issue considered in the first year of this research effort concerned possible adverse facility effects on the existing swept interaction database. In other words, do the particular characteristics of the experimental facility in which such research is conducted bias the results? In the past there have been few opportunities to perform duplicate tests in different facilities, so this question has remained open (though gross facility effects would probably have been noticed in the database). Because two members

of the Penn State Gas Dynamics Lab (G. S. Settles and F. K. Lu) were formerly involved in the AFOSR-supported research on swept interactions conducted at Princeton University during 1977-83, a unique opportunity arose to perform a facility check by repeating some of the Princeton experiments at Penn State.

Penn State Gas Dynamics Lab Experiments

The Penn State Supersonic Wind Tunnel (Fig. 1) is of an intermittent blowdown type with a test section size of 15x17 cm. It has a nominal Mach number range of 1.5 to 4.0. This variable Mach number capability is achieved by way of an asymmetric sliding-block nozzle. (Further description of the wind tunnel and the experiments can be found in Lu²).

For the present tests, a flat plate 50 cm long, spanning the tunnel, was mounted in the test section to provide the interaction test surface. A fin model with a 10° sharp leading edge was placed with its tip 216 mm from the plate leading edge and 26 mm from the tunnel sidewall (Fig. 2). The fin was 10 cm high, 127 mm long and 6.4 mm thick. The fin height of about 30% was found sufficient to ensure that the resulting shock/boundary-layer interaction was a semi-infinite one within the confines of the wind tunnel test section. The length of the fin was chosen to provide the maximum interaction extent while allowing sufficiently large angles-of-attack to be obtained without stalling the wind tunnel.

The fin was held tightly onto the flat plate by a fin-injection mechanism mounted on the tunnel sidewall. A rubber seal at the bottom of the fin ensured that no leakage under the fin occurred during the tests. The fin-injection mechanism pneumatically injected the fin to a preset angle-of-attack, α , once test conditions were established. This was necessary only for tests with α larger than approximately 14°. At lower angles, α was fixed before the run. In the experiments, α ranged from 4° to 22°, the largest value being limited by tunnel stall. The fin angle was determined to 0.1° accuracy using a machinist's protractor.

The Mach numbers of the experiments were 2.47, 2.95, 3.44, and 3.95. The incoming freestream conditions at these Mach numbers are summarized in Table 1. Since the wind tunnel is a blowdown type, the stagnation temperature decreased somewhat during a run. Typically, for a run of about twenty seconds, the stagnation temperature, T_o , dropped from 300 K to 290 K. The nominal freestream unit Reynolds number was held relatively constant throughout the Mach number range at 50 to 80 million/meter. In order to achieve this, the tunnel stagnation pressure, p_o , had to be increased with Mach number, as can be seen from Table 1.

Fig. 3 is an example of an undisturbed centerline boundary-layer velocity profile in law-of-the-wall coordinates. This figure also shows a wall-wake-law curvefit to the data. Detailed surveys along the flat-plate centerline and 38 mm to each side showed that the boundary layers were two-dimensional, turbulent, and in equilibrium at the test region and were at approximately adiabatic conditions. A summary of the incoming boundary layer conditions for the Penn State experiments is given in Table 2.

Princeton Gas Dynamics Lab Experiments

The Princeton experiments, carried out previously under AFOSR Contract F49620-81-K-0018, were run in a 20x20 cm supersonic blowdown facility at Mach 2.95 and stagnation pressures in the range of 6 to 7 atmospheres. A flat plate installation very

similar to the one described above was used. The 23 cm distance from flat-plate leading-edge to fin leading edge was essentially the same as in the present study. Thus, incoming boundary-layer thicknesses and profiles were closely comparable in both the Princeton and Penn State experiments.

Fin angles-of-attack of 5° , 9° , and 15° were tested at Mach 2.95 at Princeton. The stagnation temperature was $261 \text{ K} \pm 4\%$, and the nominal freestream Reynolds number was 63 million/meter. A more thorough discussion of these experiments can be found in Ref. 3.

Comparison of Results

The nearly-identical test conditions of the two sets of experiments described above affords a unique opportunity for comparison and the assessment of possible facility influences on swept interaction experiments. This comparison has been made under conditions of:

- *same test geometry (sharp fin)
- *same Mach number (2.95)
- *same Reynolds number (about 60 million/m)
- *same investigators (Settles & Lu)
- *different wind tunnel facilities

Detailed comparisons of the salient features of "footprints" of similar interactions studied at Penn State and Princeton have shown very close agreement. (These comparisons have been made in terms of the conical angles describing the upstream influence, primary separation, and attachment lines, and are quantitative in nature.) This result is shown by example in Fig. 4, where the Princeton and Penn State kerosene-lampblack surface-flow traces are compared for the case of a Mach 2.95, $\alpha = 9^\circ$ interaction. Other than differences arising due to the flow visualization technique itself, the two results shown are identical. *We thus conclude that facility effects are not a problem worthy of further concern at this time.*

2) Mach Number Effects

Fin-generated interactions have been relatively well studied at Mach 3 (see Refs. 1 and 3). However, no comprehensive study had been done previously over a broad Mach number range. The effect of Mach number on the interaction was therefore largely unknown. Previous studies, ranging from Mach 2 through 11, are generally inadequate for this purpose from our present standpoint, being too diverse in their quality, commonality of data obtained, and ancillary test conditions to form a coherent picture of Mach number effects. In addition, most fin interaction studies were done at one or two Mach numbers only, and were thus unable to reveal Mach number trends. Some studies were also contaminated by wind-tunnel sidewall interference or were carried out within the inception zone of the interaction. Data from such experiments obviously cannot be correlated using the otherwise powerful concept of conical symmetry¹.

A broad new experimental program was therefore devised to explore fin-generated interactions through a Mach number range of 2.5 to 4. Concurrently, computations were

performed (under separate support by C. C. Horstman of NASA-Ames Research Center) to judge the ability of the state-of-the-art computational techniques to simulate such flows. The computations were then compared with the experiments. This dual study was designed to address the following important issues:

- *the dependence of the interaction length scales on M_∞ and shock strength
- *the behavior of the conical region with Mach number change
- *the effect of Mach number on surface pressure distributions
- *the changes of the flowfield with Mach number, and
- *the ability of computational models to predict the interaction

The first phase of this research program was an analysis of the farfield upstream-influence line as revealed by surface-flow visualization. This is taken as the most salient indication of interaction "size," and thus a proper place to begin in understanding Mach number effects on swept interactions.

Using the apparatus described in the previous section of this Report, we have completed experiments to characterize the fin interaction "footprint" over the ranges $2.5 \leq M_\infty \leq 4$ and $4 \leq \alpha \leq 20$ degrees. The data set consists of surface streakline flow visualization traces and surface pressure distributions. From the former, the flow angles β_U , β_{S1} , β_{A1} , etc., describing the interaction size and strength in conical coordinates, have been extracted.

The complete details of this work may be found in Refs. 2 and 4. Here, only a brief summary of key results on the issue of Mach number effects is given. These key results may be summarized succinctly as follows:

- * conical symmetry holds for fin interactions, $2.5 \leq M_\infty \leq 4.0$
- * compressibility effects on interaction turbulence are almost nil
- * an improved interpretation of upstream influence behavior has been found

As first shown by Settles and Lu³, fin-generated interactions at Mach 3 display quasiconical symmetry about a virtual origin slightly upstream of the fin leading edge. The present work extends that principle to the range $2.5 \leq M_\infty \leq 4.0$, demonstrating that quasiconical symmetry is an inherent property of such interactions, independent of Mach number. Further, this work amounts to an extension of the conical similarity principle³ to variable Mach number.

The extension of conical similarity to include variable Mach number is based on a comparison of the upstream-influence-angle results with Mach number variation "removed" by referencing them to the freestream Mach angle, μ_∞ . When this is done, as shown in Fig. 5 (where $\beta_u \equiv \beta_u - \mu_\infty$), a barely-perceptible Mach number trend still remains. Having removed the inviscid influence of Mach number, what remains can only be the effect of compressibility on turbulence in the interaction, *ie* on its viscous nature. Fig. 5 shows that this effect is negligible. We may thus conclude that *Morkovin's Hypothesis (ie, density fluctuations play a passive role in turbulent flows below Mach 5) definitely holds for swept shock/boundary layer interactions over the ranges studied here.*

Also, a serious misconception in earlier interpretations of swept interaction upstream influence data has been corrected. Earlier investigations¹ over limited ranges of shock strength at a single Mach number (usually Mach 3) modeled the upstream influence as a

linear function of shock strength according to the following equation, where k_1 and k_2 are constants and β_0 is the fin shock angle:

$$\beta_u = k_1 \beta_0 - k_2 \quad (1)$$

This model was unsatisfactory in that Eqn. (1) did not meet the required boundary condition: $\beta_u \rightarrow \mu_\infty$ when $\beta_0 \rightarrow \mu_\infty$. Investigators at the time speculated that strange things were happening at low shock strengths, where it was believed that swept interactions were growing rapidly and nonlinearly.

The present results show that this was a misconception. The data set obtained under the subject AFOSR Grant includes data over a much wider range of combined shock strength and Mach number than in earlier studies. When the variation of upstream influence is examined vs. shock strength, as shown in Fig. 6, it becomes clear that this variation is always nonlinear. Further, one also sees that the data pass smoothly through the origin; there is no strange behavior for low shock strengths, as was previously thought. The solid line in Fig. 6 is a least-squares polynomial regression of the data, given by:

$$\beta_u = k_1 \beta_0 - k_2 \beta_0^2 \quad (2)$$

where $k_1 \approx 2.2$ and $k_2 \approx 0.027$ for the present results over the stated Mach number range. For extremely weak interactions (β_u and $\beta_0 \rightarrow 0$) an initial quasilinear growth pattern is revealed. This suggests that a linearized approach to the equations of motion might be effective in such limiting cases.

In summary, this study has gained a better physical understanding of this aspect of swept interaction behavior, and has removed a significant misconception left by the previous work.

3) Optical Flowfield Structure Results

Pulsed-Laser Holographic Interferometry Results

The flowfield structure of swept shock wave/turbulent boundary layer interactions generated by a fin mounted on a flat plate at Mach 2.43 and 2.97 has been visualized and measured by pulsed-laser holographic interferometry. The interactions studied range from moderate strength (Mach 2.43, $\alpha = 10^\circ$) to a strong case (Mach 2.97, $\alpha = 20^\circ$) with obvious flow separation. A conical holographic object beam, focused at the virtual origin of the interaction and aimed along the swept shock wave, was required to view these quasiconical interactions properly.

The sidewalls of the Penn State Supersonic Wind Tunnel required extensive optical access for the present study. The sidewall nearest the fin was fitted with a 23-cm-dia. optical glass window centered near the plate leading edge. The other sidewall was replaced by a full-coverage 20 x 50 x 4-cm-thick acrylic plastic window. Optical beams entered the flow through the glass window and exited through the acrylic window. In this way, an extensive facility modification was made in order to provide the optical access which was lacking in previous studies, and which was absolutely necessary in order to allow the present optical study of the interaction structure.

An Apollo Lasers, Inc. Model 22HD pulsed-ruby laser provided the light source for holographic interferometry. This laser was used in single-pulse mode, producing a pulse of up to 0.3 J energy and 20 nanosecond duration. A 1.2 x 2.4 m optical table was positioned beneath the wind tunnel test section in order to support both the laser and its associated optics rigidly. A 15 mW helium-neon laser, aimed through the ruby-laser cavity, was used for optical setup and alignment.

As discussed earlier, dimensionless fin-generated interactions in general display an inherent quasiconical symmetry about a virtual origin located slightly upstream of the fin leading edge. This is indicated by the sketch of the "footprint" of the fin shock in Fig. 2. The various topological features of the flow, including the upstream influence, separation, and attachment lines and the undisturbed fin shock wave itself, all converge upon a common point known as the virtual conical origin (VCO). In the near-field of the fin leading edge a systematic deviation from this conical behavior occurs, which is known as the "inception zone." Outside the inception zone, in the farfield of the interaction, all features behave conically with respect to the VCO. Briefly, this behavior has been experimentally confirmed for both the surface footprints and flowfields of a variety of swept interactions, and has further been theoretically justified.¹

Quasiconical interaction symmetry provides several immediate simplifications in studies of swept interactions: First, the natural coordinates of such interactions are spherical polar coordinates centered about the VCO (or, to a first approximation, Cartesian coordinates rotated so as to be normal and tangential to the swept shock wave). Second, outside the inception zone, the interaction structure must be purely a function of angular rather than linear dimensions; it becomes truly dimensionless. As demonstrated repeatedly,¹ all farfield measurements of a flow quantity at various distances from the fin leading edge may thus be collapsed onto a single curve.

For the optical study of such flows, the natural approach is to aim a conical light beam along the shock wave with its focus at the VCO, thus aligning the optical rays with the generating rays of the interaction. Of course, the inception zone is non-conical but its deviation from conicity is typically not large, so that it produces only a second-order effect. Schmidt and Settles⁵ have shown conical beam probing to be an excellent approximation under such conditions.

For the present experiments, the object beam of the holographic interferometer has thus been arranged to focus at or near the VCO, and to be aimed along the sweep line of the main fin shock. A diagram of this arrangement is given in Fig. 7, where a top view of the test section and optics is shown for clarity.

AGFA 8E75 holographic plates of 10 x 12.5 cm size were positioned outside the acrylic window and normal to the object-beam axis. During wind-tunnel tests with continuous helium-neon laser illumination, the object beam was aligned with the flow so as to cast a shadowgram of the conical interaction at the position of the holographic plate. Interferograms were then exposed by pulsing the ruby laser once with flow off and again with flow on, the only optical path change being thus due to the flow itself. There was initial concern about possible spurious fringes due to wind tunnel vibration between exposures, but this proved not to be a problem so long as all optical components were rigidly mounted. The developed plates, being practically equivalent to image-plane holograms, were reconstructed by a simple white-light procedure.⁶

This arrangement for holographic interferometry by taking advantage of the natural symmetry of a swept interaction has never been done before to our knowledge. The

reasons include both ignorance of the proper coordinate frame and the extreme demands this approach places on optical access to a test facility. Previous attempts at optical probing of swept interactions with parallel light normal to the wind tunnel axis have been fruitless. However, the proper approach was appreciated by Zubin and Ostapenko,⁷ who performed conical shadowgraphy of swept interactions under test conditions similar to those of the present study.

Given windows positioned properly to allow the necessarily skewed viewing angles, the major difficulty of this approach lies in proper beam alignment. When perfectly aligned as shown in Fig. 7, the conical holographic interferometer is partially blocked by the leading edge of the fin itself, so that no features of the interaction downstream of the shock wave may be observed. Further, experiments showed that the proper position for the beam focus lies precisely on the flat plate surface, and that any vertical misalignment above this point degrades the results. (Horizontal misalignment away from the true VCO also has a similar effect.)

Unfortunately, perfect object-beam alignment was not possible in the present study. Horizontal misalignment toward the lower right-hand direction in Fig. 7 was done deliberately in order to see the important features of the interactions aft of the fin shock. Some vertical misalignment (along the outward normal direction with respect to Fig. 7) also appeared necessary in order to avoid serious beam distortions caused by reflecting the object-beam focus directly off the surface of the flat plate. As a result, conical shock-wave surfaces appear slightly spread-out rather than sharp in the holographic interferograms, since these surfaces are viewed not exactly edge-on.

Several possible solutions to these alignment problems were contemplated. Providing the fin leading-edge with a small transparent window (about 5 mm dia.) to pass the object beam, or cutting a small notch in the leading edge, are horizontal-misalignment solutions which generate further problems of their own. A simpler, interim solution was found late in the present test series by positioning the object beam focus exactly at the fin leading-edge rather than at the VCO, so as to avoid beam blockage by the fin. This approach works according to the rule discovered by Schmidt and Settles,⁵ that axial misalignment is relatively innocuous compared to transverse (horizontal or vertical) displacement in conical shadowgraphy. In any case, the results discussed earlier show that the fin leading-edge and the VCO become practically coincident for sufficiently high interaction strength.

As for vertical misalignment, there seems to be no other solution than to reflect the object-beam focus from the surface of the flat plate. Accordingly, a high polish on the plate in the vicinity of the fin leading-edge is desirable for specular reflection.

A thorough discussion of the results of the present conical holographic studies of swept interactions is presented in Refs. 6 and 8. Here, two examples will be shown with comparisons to previous flowfield measurements and computations.

Oskam⁹ produced the first detailed fin-interaction surveys for $\alpha = 4^\circ$ and 10° at $M_\infty = 2.95$. For the latter case, his plot of the interaction structure is reproduced here in Fig. 8a, along with the corresponding holographic interferogram from the present work. Oskam's incoming boundary layer was considerably thicker than the present one, though his freestream Reynolds number was comparable to ours. According to the established Reynolds-number scaling law,¹ Oskam was thus close to the fin leading-edge in non-dimensional terms, and probably within the inception zone. Other than that, a direct comparison may be made between his results and the present results in Fig. 8a.

The rear shock of the λ -foot bifurcation is not adequately resolved in Oskam's

results, though it appears clearly in the holographic interferogram of Fig. 8a. However, the slip line and the lifting and subsequent impingement of the separated shear layer beneath the λ -foot are, in retrospect, shown quite clearly. Oskam indicated the presence of wave phenomena in the aft region of the interaction (especially above the slip line) which are not supported by the present flowfield model. His assertion that flow separation did not occur in this interaction, later voiced by Bogdonoff¹⁰ for swept interactions in general, is now widely recognized to be incorrect. However, in Oskam's defense, his early work considered a particular interaction of only moderate strength (ie $M_\infty = 2.95$, $\alpha = 10^\circ$) in which the flow separation was not obvious, given the resolution of his cobra-probe instrumentation.

Fig. 8b reproduces the computed pitot-pressure contour plot of Zang and Knight¹¹ for $M_\infty = 2.95$, $\alpha = 17.5^\circ$, compared with the present holographic interferogram for the same Mach number and $\alpha = 20^\circ$. An immediate conclusion is that, within the separated region where the grid density was high, the computed results appear quite reasonable. However, the coarser grid above this region has failed to resolve any details of the λ -foot, transonic jet, or slip line. This is not an indictment of the computation, which pushed the limits of current supercomputer speed and storage in any case. Nonetheless, a key question is raised: How much of the interaction structure can be lost due to inadequate grid resolution without compromising the integrity of the entire solution?

Some index of the interaction strength is required in order to relate such interaction cases at different M_∞ and α . For this purpose, note that the interaction structural view shown is one *normal* to the fin shock, with the normal component of the incoming stream entering from the left and the sense of the tangential flow being directed into the page. As indicated earlier, this is the natural coordinate frame for the study of these essentially-conical flowfields. Such swept interactions may be correctly described as "conically transonic," in that the flow in the normal plane is transonic (due to sweepback) despite the supersonic freestream Mach number. The point is made that the normal Mach number is the sought-for index of interaction strength for swept interactions.¹

Fig. 9 is a plot of the static pressure ratio across the main fin shock as a function of M_n , with points shown for all seven of the current test conditions. Indications of the approximate interaction strengths for incipient primary and secondary boundary-layer separation are also shown, based on the empirical criteria of Korkegi and of Zheltovodov.¹

Fig. 9 shows that the current test conditions span the range from a moderate-strength case just beyond incipient primary separation ($M_\infty = 2.43$, $\alpha = 10^\circ$) to the strong interaction at $M_\infty = 2.97$, $\alpha = 20^\circ$. Weaker interactions were not studied at present due to the optical limitation imposed by the downstream edge of the acrylic sidewall window described earlier.

Until recently the best-available physical model of the structure of swept, fin-generated interactions was that of Zheltovodov,¹². Though accurate up to the rear shock of the λ -foot, his model is confused in the region between the rear shock and the fin. Present results demonstrate that the flow in this region is dominated by a jet emanating from the λ -foot and impinging on the flat plate just ahead of the fin. These results further allow an even more detailed model to be constructed. Using the Mach 2.97, 20° interaction as an example, a true-scale diagram of the interaction structure is shown in Fig. 10.

In Fig. 10 the incoming boundary layer δ separates from the flat plate at the location denoted by conical angle β_{s1} . (A small upstream influence region ahead of separation is not shown in the Figure.) The separated turbulent shear layer is turned upward by the separation shock, thence downward by the rear shock. This shear layer turns rapidly toward the flat plate, where it impinges. The resultant spreading of skin-friction lines on the

surface is denoted by the angle β_{a1} . The reverse flow at $\beta > \beta_{a1}$ feeds a spiral separation vortex centered roughly beneath the rear shock.

Between β_{a1} and β_0 the reversed flow forms a new boundary layer on the flat plate. This boundary layer grows and encounters first a favorable and then an adverse pressure gradient as it travels forward. For sufficiently-strong interactions (see Fig. 10), a secondary separation of this reversed boundary layer occurs at β_{s2} . In the present experiments this feature is weak but definitely present. Finally, following secondary separation and its associated attachment (not shown in Fig. 10 due to the small scale involved), the reversed boundary layer proceeds forward to β_{s1} . All the while, the reversed flow contributes by turbulent entrainment to the vortex and the separated shear layer above it.

Since the rear shock does not penetrate into the separation vortex, one may presume that a sonic line exists along the underside of the separated shear layer, and that the entire separation zone is subsonic in the normal plane for present test conditions. Zubin and Ostapenko,⁷ however, found evidence to support possible supersonic reversed flow for even stronger interactions.

The incoming-flow streamtube subtended by the separation shock is processed through it and the rear shock of the λ -foot. Aft of the rear shock, this streamtube is bounded below by the separated turbulent shear layer and above by a slip line emanating from the triple-point shock intersection. The rear shock, by virtue of its near-normal angle to its incoming flow direction, is clearly a strong oblique shock with a subsonic outflow condition. However, the presence of a Prandtl-Meyer expansion fan immediately downstream of the rear shock indicates that the flow reaccelerates through a sonic line there. The Prandtl-Meyer fan reflects from the slip line as a compression which coalesces into a transonic shock train centered in the separated shear layer as it turns toward the plate. Decelerated to subsonic conditions by this shock train, the streamtube composed originally of outer inviscid flow impinges in a jet-like manner upon the flat plate between β_{a1} and the fin.

The slip line itself must necessarily begin as a laminar free shear layer at the triple point. It is observed to undergo transition to turbulence in the vicinity of the Prandtl-Meyer fan reflection, and is clearly turbulent when it impinges near the corner of the fin and flat plate. Thus, the interaction is characterized by *two* shear layer impingements, namely, those of the slip line and the separated shear layer.

This view of the interaction flowfield structure, involving both jet and shear layer impingements on the flat plate, is thought to be responsible for the high levels of surface pressure, shear, and heat flux measured near fin/plate junctions by many investigators. This structure is fundamentally the same as that discovered by Edney¹³ for the case of jet impingement due to shock-wave interference. However, while Edney's work showed supersonic jet impingement, the present cases are all transonic in the normal plane.

Finally, it is observed that the flow aft of the main shock and above the slip line, though nonuniform, is clearly subsonic in the normal plane. No wave motion is seen there, and the Prandtl-Meyer fans in the jet region reflect from the slip line without propagating through it.

Laser-Light-Screen Results

The flowfield structure described above was also observed by the laser-light-screen (LLS) technique¹⁴, in which the beam from a 2-Watt Argon-ion laser was expanded into a thin

sheet and passed through the flow normal to the swept shock wave. Moisture was added to the airstream of the Penn State Supersonic Wind Tunnel, so that the cross-section of the airstream became visible due to Mie scattering of the laser sheet. The results were then photographed, yielding both qualitative and quantitative structural information on the flow over the parameter ranges $2.5 \leq M_\infty \leq 3.5$ and $4 \leq \alpha \leq 18$ degrees. A diagram of the experimental setup for LLS imaging of fin-generated swept interactions is given in Fig. 11.

Since laser light-screen results are inherently of low contrast, digital image processing has been used for contrast enhancement. Even so, these results do not yield the same level of detail as the conical holographic interferometry technique described above. The LLS data were, however, taken over a somewhat broader parameter range, and, in the natural order of progression of the research, they were done first.

Some previously-known features of the flowfield structure, such as the separation shock, "lambda-foot," and triple point, were clearly revealed. The evolution of these features with increasing interaction strength has been quantified¹⁴. Weak interactions appear nearly featureless, but distinct structural features appear and evolve as the shock strength increases. From these results we first observed the flowfield structure downstream of the triple-point in strongly separated interactions, which had not been observed previously.

Examples of such laser-light-screen images, with contrast enhanced by digital image processing, are shown in Figs. 12-14 (in these images the direction of flow is from right to left). Fig. 12 depicts the weak interaction produced at $M_\infty = 2.5$ by a fin angle $\alpha = 10^\circ$. Little detail is evident here, compared to the holographic interferogram taken under the same conditions. However, the stronger case shown in Fig. 13 ($M_\infty = 3.5$, $\alpha = 10^\circ$) clearly reveals the λ -foot structure and the separation bubble underneath it. One of the strongest interactions observed ($M_\infty = 3.5$, $\alpha = 15^\circ$) is shown in Fig. 14, where the λ -foot, slip line and Prandtl-Meyer fans in the impinging jet are visible. The reader is referred to Ref. 14 for a detailed discussion of the analysis and results of the entire set of LLS interaction flowfield images obtained in this study.

Conical White-Light Shadowgraphy Results

Near the conclusion of the subject Grant, a strobed white-light source was substituted for the pulsed laser source in the conical imaging scheme of Fig. 7. By applying the alignment scheme discussed earlier (wherein axial misalignment is permitted by transverse misalignment is avoided), it was possible to obtain perfectly-aligned flowfield images on both photographic and videotape media. Only one interaction was so observed: the strong case which occurs at $M_\infty = 3.0$, $\alpha = 20^\circ$. A conical shadowgram of this case is shown in Fig. 15. The extraordinary level of clarity and detail shown here were primarily responsible for the flowfield model shown earlier in Fig. 10, which is based on this particular example from the overall test matrix.

4) Laser Interferometer Skin Friction Results

During the period 1983-1986, a new instrument for compressible-flow skin friction measurement—the Laser Interferometer Skin Friction (LISF) meter, was developed at the Penn State Gas Dynamics Laboratory¹⁵. This instrument, which operates on the principle

of optical measurement of the thinning of an oil film on a polished surface undergoing aerodynamic shear, was at the time (and perhaps still is) the only instrument of its type in the world. Its development was undertaken prior to the present AFOSR Grant, and was funded primarily by the NASA-Lewis Research Center.

Subsequently, measurements by the LISF meter of the Mach 3, $\alpha = 10^\circ$ and 16° and Mach 4, $\alpha = 16^\circ$ and 20° fin interactions have been successfully carried out in the Penn State Supersonic Wind Tunnel. In order to carry out these experiments it was necessary to configure the LISF instrument to look directly down on the flat plate test surface from above, as illustrated in Figs. 16-18. Also, a replacement test section ceiling was designed and constructed to contain the plexiglass window needed for optical observation from above. Having made the necessary modifications to the LISF instrument and tunnel ceiling, kerosene-lampblack surface flow visualization traces of the Mach 3, $\alpha = 10^\circ$ and 16° fin interactions were taken to recheck the flow quality, which was found to be quite good.

Since LISF measurements are pointwise and time-consuming, some consideration was given to the proper location of the measuring positions on the flat plate. First of all, since no skin friction data of established accuracy exist for any swept interaction, it was desired to produce data which will serve as a "benchmark." It thus seems reasonable to acquire data in the region from the undisturbed boundary layer to the fin in the zone of quasiconical flow symmetry, *ie*, outside the interaction inception zone. (Measurements inside the inception zone provide less general information, thus are assigned a lower priority.) Secondly, one thus makes use of the inherent symmetry of the interaction, which calls for a spherical polar system of coordinates. For surface measurements, such coordinates form concentric circular arcs centered about the virtual conical origin of the flow. However, it was our intention to measure interactions of different α in this way, and the virtual origin changes with α . Since the virtual origin is not far displaced from the fin leading edge, the latter has been chosen as the origin of coordinates for simplicity.

The chosen datum radius for detailed skin friction data in the Mach 3, $\alpha = 10^\circ$ fin interaction was 114 mm from the fin leading edge. This was chosen to be well downstream of the inception zone according to the established scaling law for that zone¹:

$$(L_i/r_o)Re\delta_o^a = k_1 \tan\lambda_s \quad (3)$$

where $a \approx 1/3$ at Mach 3, $k_1 \approx 1100$, and λ_s is the sweepback angle of the fin shock. For our current tests at $Re = 5.9 \times 10^7$ /meter and $\delta_o = 4.2$ mm, Eqn. 3 yields an inception length L_i of about 5 cm from the fin leading edge. By making use of the quasiconical symmetry of the interaction, it is possible to plot the LISF data vs. angle β from the freestream direction. The results will thus automatically be in dimensionless coordinates (as, indeed, all conical flows must be).

The LISF skin friction data for the Mach 3, $\alpha = 10^\circ$ and 16° interactions are shown in these coordinates in Figs. 19 and 20. Also shown are the Navier-Stokes computational prediction¹⁶ of Horstman (private communication) and Knight¹⁶. Figs. 19 and 20 are very revealing and bear some discussion.

First of all, the reason to obtain LISF data is that there is no other known technique which will measure skin friction with predictable accuracy in a shock/boundary layer interaction. The Preston-tube method is much simpler to use than LISF, but does not actually measure skin friction. Instead, it measures pitot pressure at the wall and infers skin

friction through a calibration which cannot be trusted in a strongly-interacting flow. Further, reliable skin friction data are sorely needed to test the predictive capabilities of current Navier-Stokes solvers. Here, representative state-of-the-art computations are tested against reliable data with an established accuracy of $\pm 5\%$.

In brief, it appears from Figs. 19 and 20 that both computations have done well for Mach 3 interactions of moderate strength. Both Knight's and Horstman's CFD results are in good agreement with the LISF skin friction measurements at both fin angles of attack. A complete discussion of this result, as well as of the LISF instrument and the experiments described above, is included Ref. 16, to which the reader is referred.

Unfortunately, the CFD predictive ability breaks down for the stronger interactions surveyed by LISF at Mach 4. Figs. 21 and 22 show the Mach 4, $\alpha = 16^\circ$ and 20° skin friction data in comparison with computed results by Horstman (as yet unpublished; Knight has yet to compute these cases). The peak skin friction value near flow reattachment in these strong interaction cases is highly exaggerated, and is underpredicted by as much as 100% in the computational results.

Fig. 23, which is a plot of $c_{f,peak}/c_{f\infty}$ vs. the static pressure ratio across the fin shock, reveals the dramatic failure of the computational predictive ability with increasing interaction strength. However, whether this failure is due solely to increasing interaction strength (*ie* at any Mach number), or whether it is perhaps due to the jump from Mach 3 to Mach 4, is still an open question. Results from the Mach number effects study described earlier in this Report cast doubt on the latter hypothesis, but LISF measurements for stronger interactions at Mach 3 will be required to resolve this issue.

IV. Conclusions & Recommendations for Future Work

This Final Technical Report on AFOSR Grant 86-0082 has reported an experimental research effort of the Penn State Gas Dynamics Laboratory on the subject of swept shock wave interactions with turbulent boundary layers. The research relied largely on non-intrusive, laser-based optical flow diagnostics. Results have revealed the Mach number influence on fin-generated swept interactions over the range of Mach 2.5 to 4.0, showing that this influence is primarily inviscid and that, contrary to previous hypotheses, the development of these interactions follows a smooth (though nonlinear) continuum. Important discoveries have been made about the detailed flowfield structure of such flows, showing that they are dominated by a jet-impingement phenomenon arising from the bifurcation of the incident shock wave due to boundary-layer separation. Quantitative skin friction measurements of fin-generated swept interactions over the supersonic range, including weak, moderate, and strong interactions, have been presented. High skin friction levels were measured in the vicinity of the jet-impingement zone, and were used for the validation of computational predictions carried out by others. The results of this code validation exercise appear to show a systematic breakdown in the predictive ability of state-of-the-art CFD methods with increasing interaction strength.

In terms of the skin friction issue, measurements are needed for stronger interactions at Mach 3 in order to resolve a question still remaining about the relative effects of Mach number and interaction strength.

Given the successful demonstration of conical optical flow diagnosis of these interactions, a wide variety of useful experiments can now be done. With proper alignment, holographic interferometry can now be used to obtain quantitative density profile data for

a wide range of interaction strengths. Similarly, the evolution of the structure of these interactions may be studied in more detail than has been possible in this initial study. Finally, the conical optical frame opens the possibility of time-resolved fluctuation measurements of the interaction flowfield, which have never been done to date, using a technique such as laser deflectometry. Such experiments would be extremely valuable in answering important questions about the steadiness of such interactions, its role in the overall interaction physics, and its effect on CFD predictive capability.

V. Publications

- 1) Hsu, J. C., and Settles, G. S., "Holographic Interferometry of Swept Shock/Boundary Layer Interactions," to be presented at the 5th Intl. Symposium on Flow Visualization, Prague, 21-25 August, 1989.
- 2) Hsu, J. C., and Settles, G. S., "Measurements of Swept Shock Wave/Turbulent Boundary Layer Interactions by Holographic Interferometry," AIAA paper 89-1849, presented at the AIAA 20th Fluid Dynamics, Plasma Dynamics, and Lasers Conference, Buffalo NY, June 12-14, 1989.
- 3) Lu, F. K., and Settles, G. S., "Color Surface-Flow Visualization of Fin-Generated Shock-Wave Boundary-Layer Interactions," to be published in *Experiments in Fluids*.
- 4) Lu, F. K., and Settles, G. S., "Inception to a Fully-Developed Fin-Generated Shock-Wave Boundary Layer Interaction," AIAA Paper 89-1850, presented at the AIAA 20th Fluid Dynamics, Plasma Dynamics, and Lasers Conference, Buffalo NY, June 12-14, 1989.
- 5) Settles, G. S., Metwally, O. M., Hsu, J. C., and Lu, F. K., "Visualization of High-Speed Flows at the Penn State Gas Dynamics Laboratory," *Proc. 1988 International Conference on Applications of Lasers and Electro-Optics*, Santa Clara, Oct. 30, 1988, Laser Inst. of America Vol. 67, pp. 95-101.
- 6) Fung, Y-T, Settles, G. S., and Ray, A., "Microprocessor Control of High-Speed Wind Tunnel Stagnation Pressure," AIAA Paper 88-2062, presented at the AIAA Aerodynamic Testing Conference, San Diego, CA, May 18-20, 1988.
- 7) Lu, F. K., and Settles, G. S., "Structure of Fin-Shock/Boundary Layer Interactions by Laser Light-Screen Visualization," AIAA Paper 88-3803, presented at the 1st National Fluid Dynamics Congress, Cincinnati, OH, July 1988.
- 8) Kim, K-S, and Settles, G. S., "Skin Friction Measurements by Laser Interferometry in Swept Shock Wave/Turbulent Boundary-Layer Interactions," AIAA Paper 88-0497, presented at the AIAA 26th Aerospace Sciences Conference, Reno, NV, January 11-14, 1988. (to be published in the *AIAA Journal*.)
- 9) Kim, K.-S., and Settles, G. S., "Skin Friction Measurements by Laser Interferometry," Ch. 3 of AGARDograph No. 315, A Survey of Measurements and Measuring Techniques in Rapidly Distorted Compressible Turbulent Boundary Layers, eds. H. H. Fernholz, A. J. Smits, and J.-P. Dussauge, November 1988.
- 10) Lu, F. K., Settles, G. S., and Horstman, C. C., "Mach Number Effects on Conical Surface Features of Swept Shock Boundary-Layer Interactions," AIAA Paper 87-1365, June 1987, (to be published in the *AIAA Journal*.)

VI. References

- 1) Settles, G. S., and Dolling, D. S., "Swept Shock Wave-Boundary Layer Interactions," in "Tactical Missile Aerodynamics," eds. M. J. Hemsch and J. N. Nielsen, Vol. 104 of *AIAA Progress in Astronautics and Aeronautics Series*, September, 1986, pp. 297-379.
- 2) Lu, F.K., "Fin-Generated Shock-Wave Boundary-Layer Interactions," Ph.D. Thesis, Mechanical Engineering Dept., Penn State University, Feb. 1988.
- 3) Settles, G. S., and Lu, Frank K., "Conical Similarity of Shock/Boundary-Layer Interactions Generated by Swept and Unswept Fins," *AIAA Journal*, Vol. 23, No. 7, July, 1985, pp. 1021-1027.
- 4) Lu, F. K., Settles, G. S., and Horstman, C. C., "Mach Number Effects on Conical Surface Features of Swept Shock Boundary-Layer Interactions," AIAA Paper 87-1365, June 1987, (to be published in the *AIAA Journal*.)
- 5) Schmidt, M. C., and Settles, G. S., "Alignment and Accuracy of the Conical Shadowgraph Flow Visualization Technique," *Experiments in Fluids*, Vol. 4, No. 2, pp. 93-96.
- 6) Hsu, J. C., and Settles, G. S., "Holographic Interferometry of Swept Shock/Boundary Layer Interactions," to be presented at the 5th Intl. Symposium on Flow Visualization, Prague, 21-25 August, 1989.
- 7) Zubin, M.A., and Ostapenko, N.A., "Structure of the Flow in the Separation Region Resulting from Interaction of a Normal Shock Wave with a Boundary Layer in a Corner," *Izvestiya AN SSSR, Mekhanika Zhidkosti i Gaza*, 3, May-June 1979, pp. 51-85.
- 8) Hsu, J. C., and Settles, G. S., "Measurements of Swept Shock Wave/Turbulent Boundary Layer Interactions by Holographic Interferometry," AIAA paper 89-1849, presented at the AIAA 20th Fluid Dynamics, Plasma Dynamics, and Lasers Conference, Buffalo NY, June 12-14, 1989.
- 9) Oskam, B., Vas, I.E., and Bogdonoff, S.M., "An Experimental Study of Three-Dimensional Flow Fields in an Axial Corner at Mach 3," AIAA Paper 77-689, June 1977.
- 10) Bogdonoff, S.M., "Some Observations of Three Dimensional Shock-Wave Turbulent Boundary Layer Interactions," IUTAM Symposium on Turbulent Shear Layer/Shock Wave Interactions, Palaiseau, France, 1985, pp. 261-272.
- 11) Zang, Y., and Knight, D.D., "Computation of Sharp Fin and Swept Compression Corner Shock/Turbulent Boundary Layer Interactions," AIAA Paper 89-1852, June 1989.
- 12) Zheltovodov, A. A., "Properties of Two- and Three-Dimensional Separation Flows at Supersonic Velocities," *Izvestiya Akademii Nauk SSSR, Mekhanika Zhidkosti i Gaza*, Vol. 14, May-June 1979, pp. 42-50.

13) Edney, B., "Anomalous Heat Transfer and Pressure Distributions on Blunt Bodies at Hypersonic Speeds in the Presence of an Impinging Shock," FFA Report 115, 1968.

14) Lu, F. K., and Settles, G. S., "Structure of Fin-Shock/Boundary Layer Interactions by Laser Light-Screen Visualization," AIAA Paper 88-3803, presented at the 1st National Fluid Dynamics Congress, Cincinnati, OH, July 1988.

15) Kim, K.-S., and Settles, G. S., "Skin Friction Measurements by Laser Interferometry," Ch. 3 of AGARDograph No. 315, A Survey of Measurements and Measuring Techniques in Rapidly Distorted Compressible Turbulent Boundary Layers, eds. H. H. Fernholz, A. J. Smits, and J.-P. Dussauge, November 1988.

16) Kim, K-S, and Settles, G. S., "Skin Friction Measurements by Laser Interferometry in Swept Shock Wave/Turbulent Boundary-Layer Interactions," AIAA Paper 88-0497, presented at the AIAA 26th Aerospace Sciences Conference, Reno, NV, January 11-14, 1988. (to be published in the *AIAA Journal*.)

M_∞	p_o , MPa (psia)	T_o , K (°R)	$Re \times 10^{-6}$, m^{-1} (/ft)
$2.47 \pm 0.1\%$	$0.54 \pm 2.0\%$ (78)	$295 \pm 0.9\%$ (531)	$53.8 \pm 0.9\%$ (16.3)
$2.95 \pm 0.3\%$	$0.76 \pm 2.7\%$ (110)	$295 \pm 0.9\%$ (531)	$58.9 \pm 1.9\%$ (17.8)
$3.44 \pm 0.2\%$	$1.03 \pm 3.0\%$ (150)	$295 \pm 0.8\%$ (531)	$64.0 \pm 1.7\%$ (19.4)
$3.95 \pm 0.4\%$	$1.58 \pm 5.0\%$ (230)	$295 \pm 1.3\%$ (531)	$75.8 \pm 1.7\%$ (23.0)

Table 1 Incoming Freestream Conditions

M_∞	2.47	2.95	3.44
δ , mm	3.60 ± 0.14	3.63 ± 0.04	3.24 ± 0.06
δ^* , mm	0.82 ± 0.02	0.93 ± 0.11	0.92 ± 0.05
θ , mm	0.22 ± 0.004	0.19 ± 0.02	0.15 ± 0.01
$c_f \times 10^3$	1.78 ± 0.07	1.64 ± 0.12	1.51 ± 0.40
Π	0.63 ± 0.25	0.58 ± 0.22	0.51 ± 0.06

Table 2 Incoming Boundary-Layer Parameters

The Penn State Variable-Mach Number Supersonic Wind Tunnel Facility

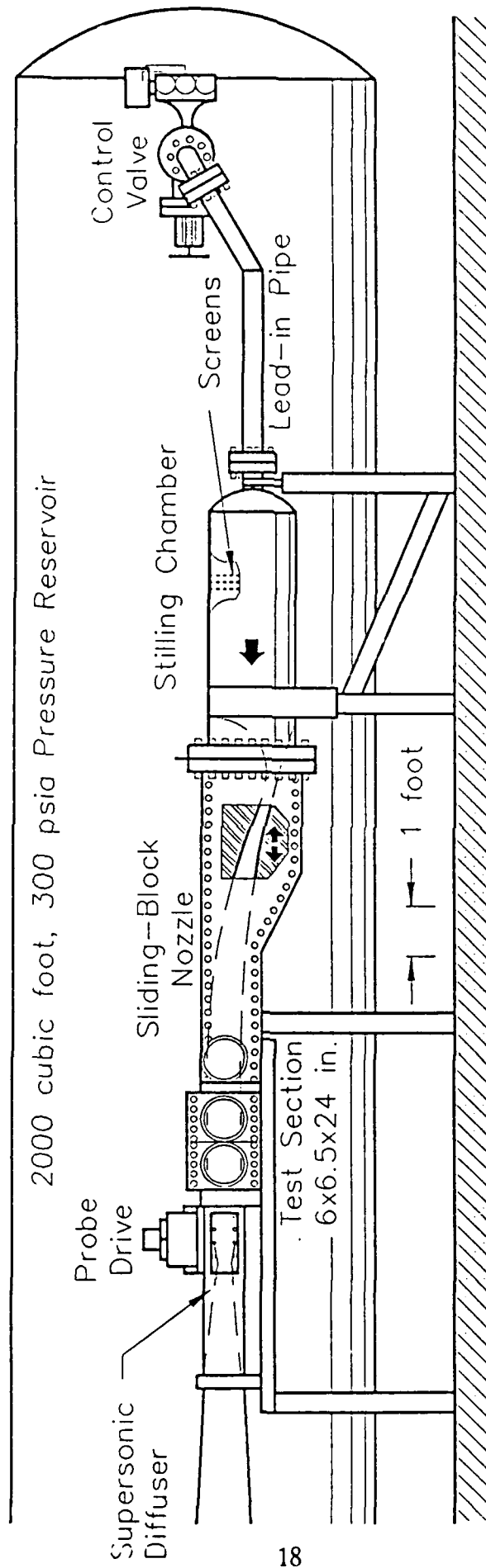


Figure 1.a. The Penn State Variable-Mach Number Supersonic Wind Tunnel Facility

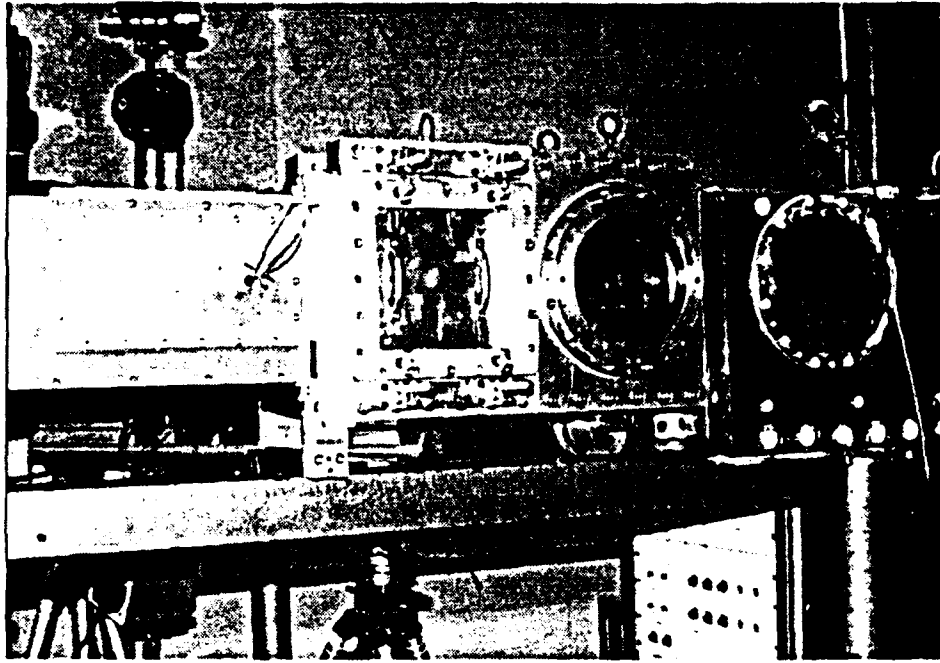


Figure 1.b. Photo of Test Section

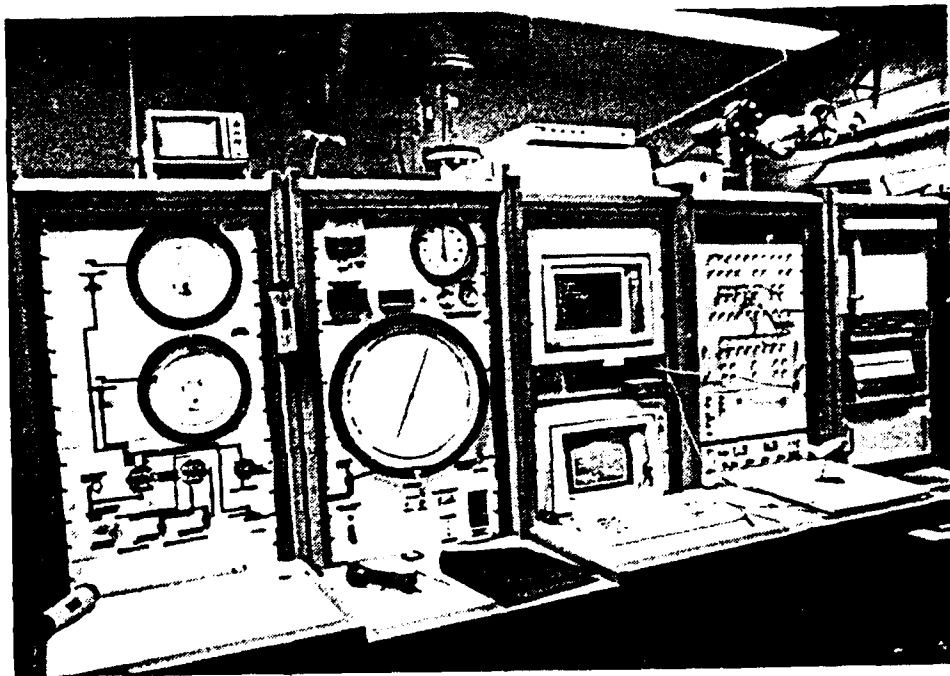


Figure 1.c. Photo of Control Console

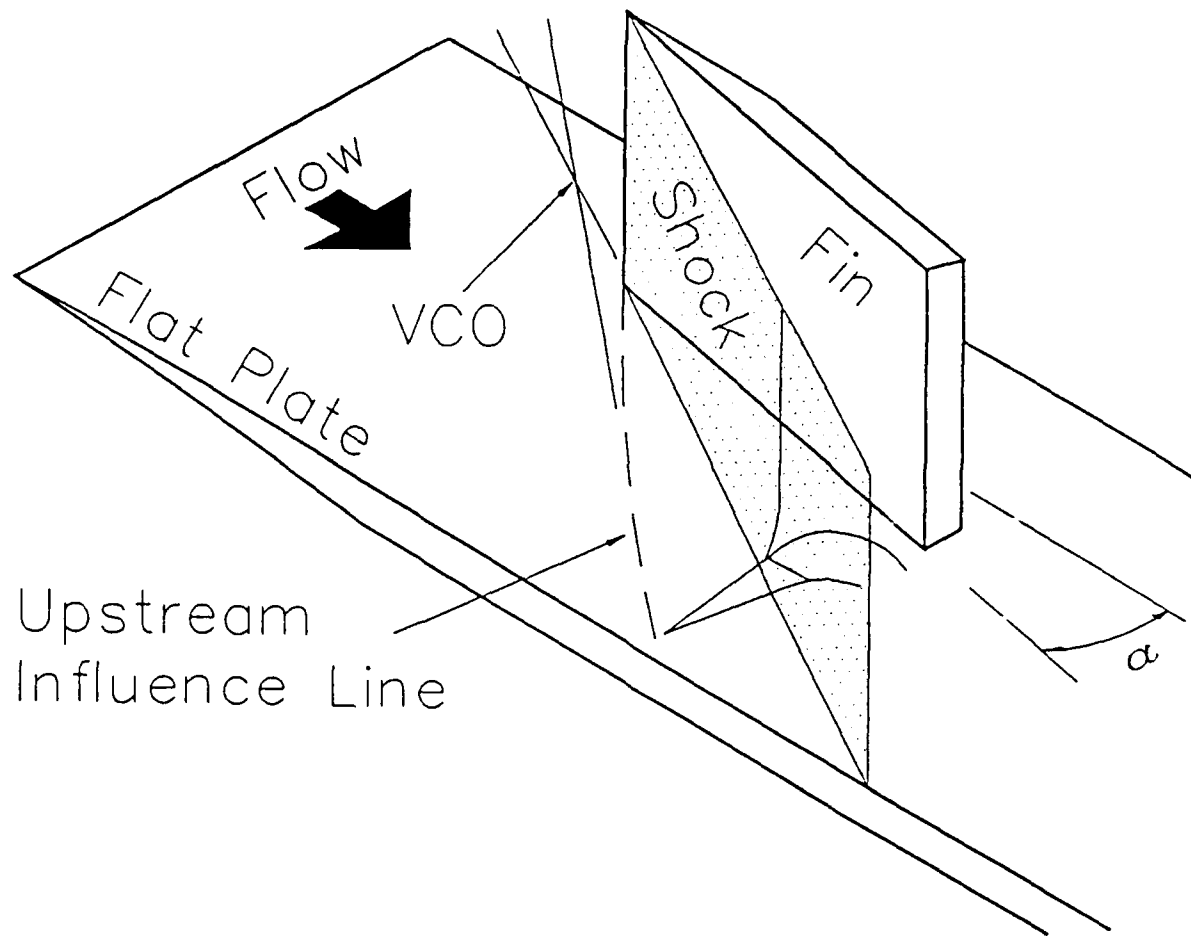


Figure 2 Diagram Of Fin And Flat Plate Installation

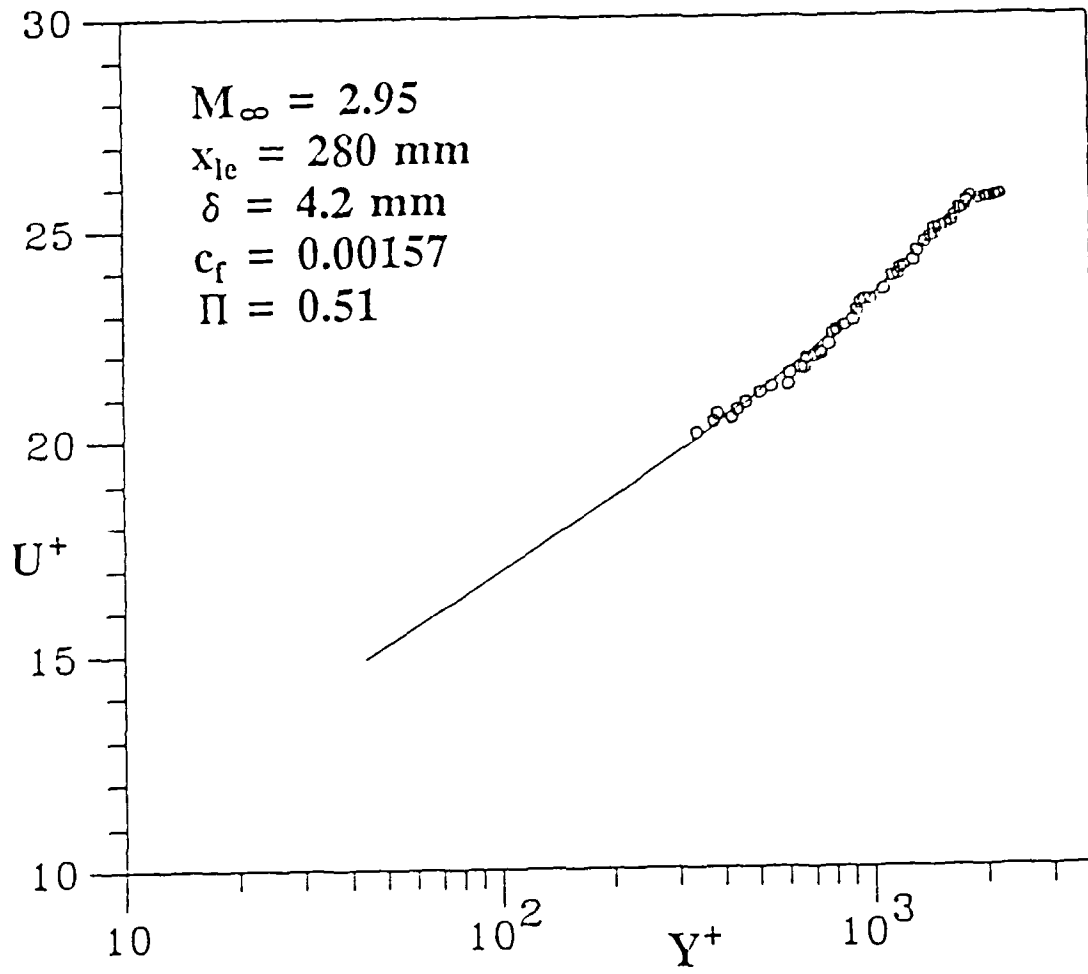
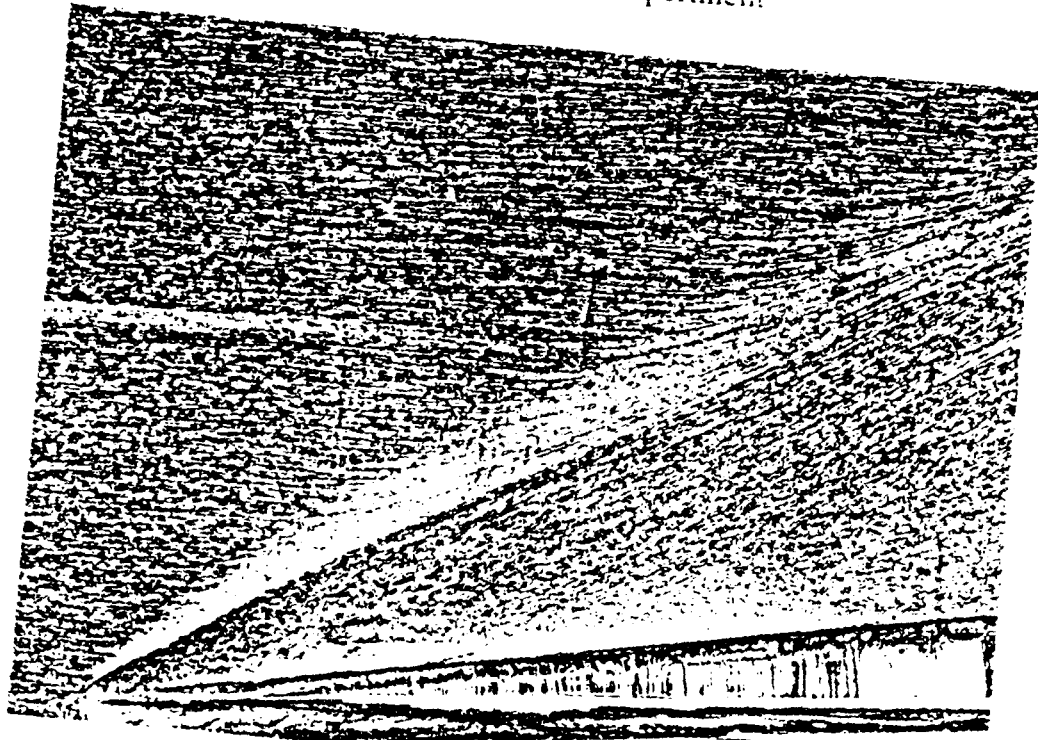


Figure 3 Typical Flat Plate Boundary-Layer Velocity Profile

a. Penn State Experiment



b. Princeton Experiment

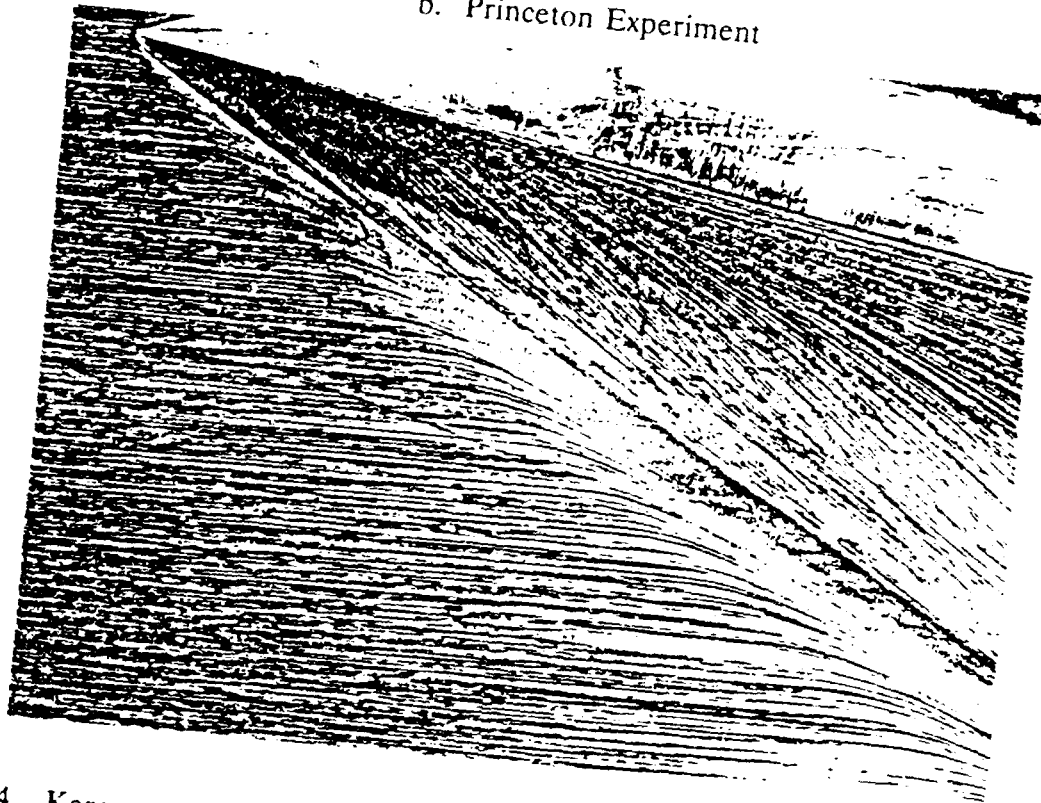


Figure 4 Kerosene-Lampblack Traces Of Fin Interaction Footprint, $M = 2.95$, $\alpha = 9^\circ$

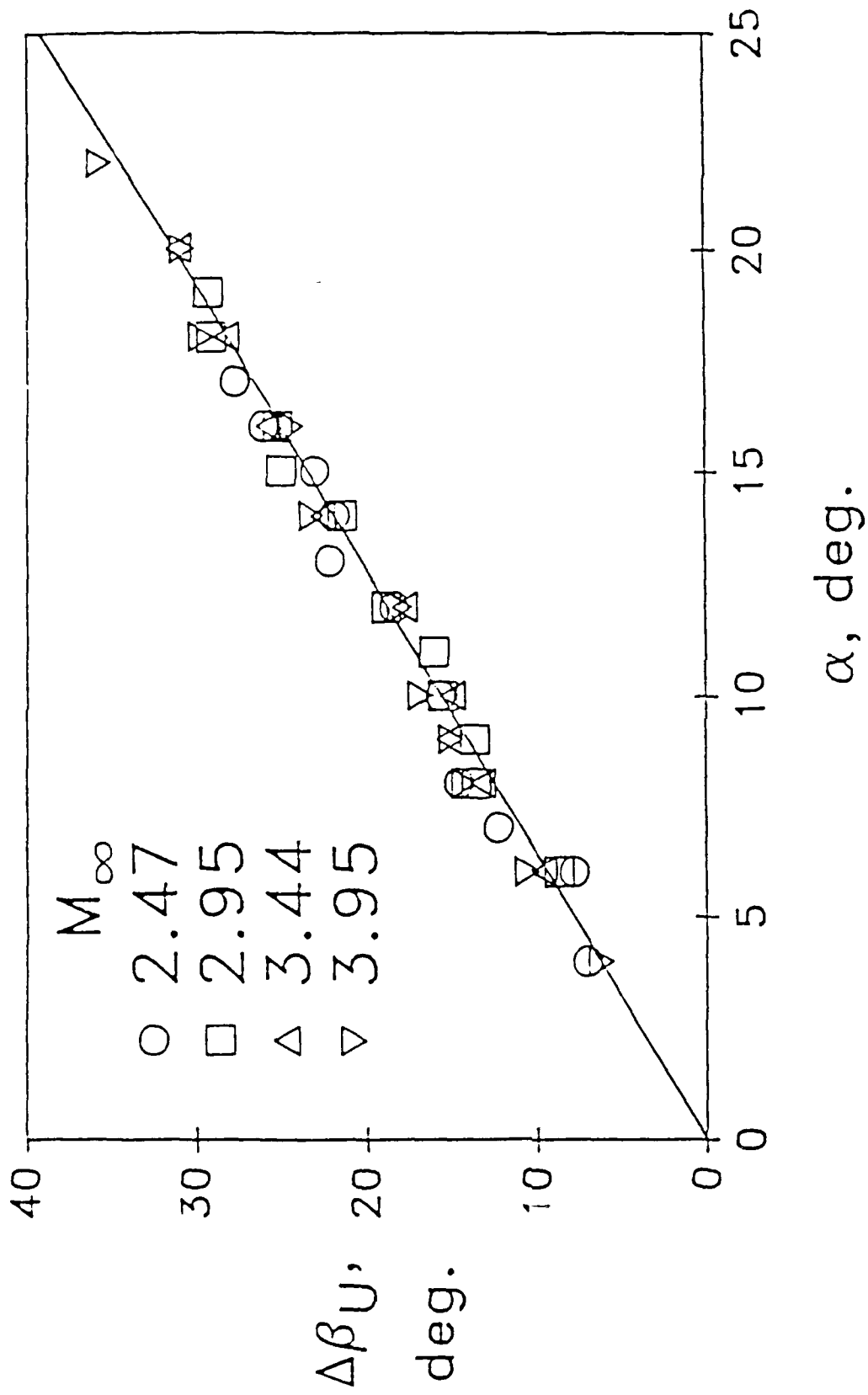


Figure 5 Reduced Upstream-Influence Angle vs. Fin Angle-Of-Attack

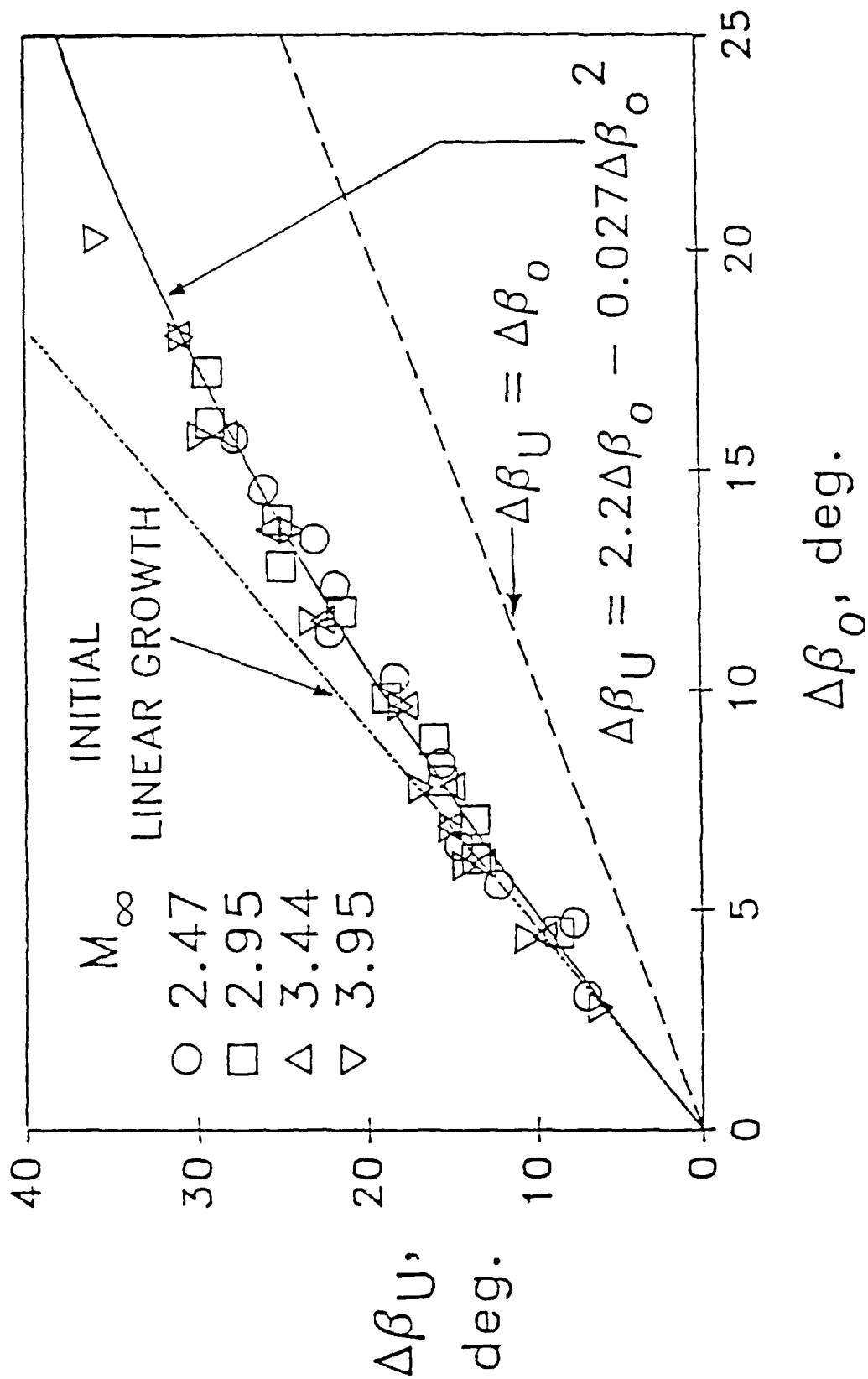
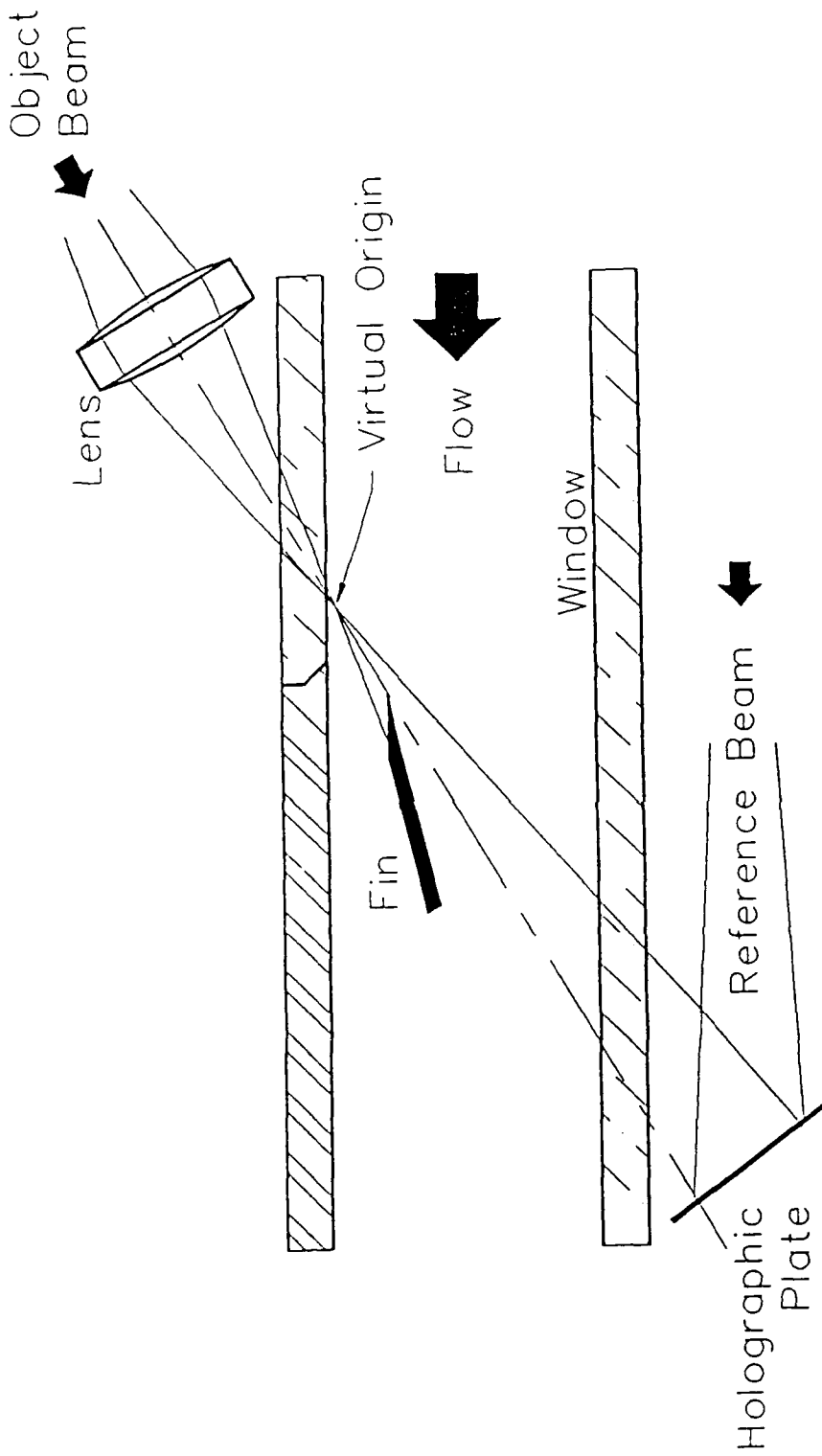
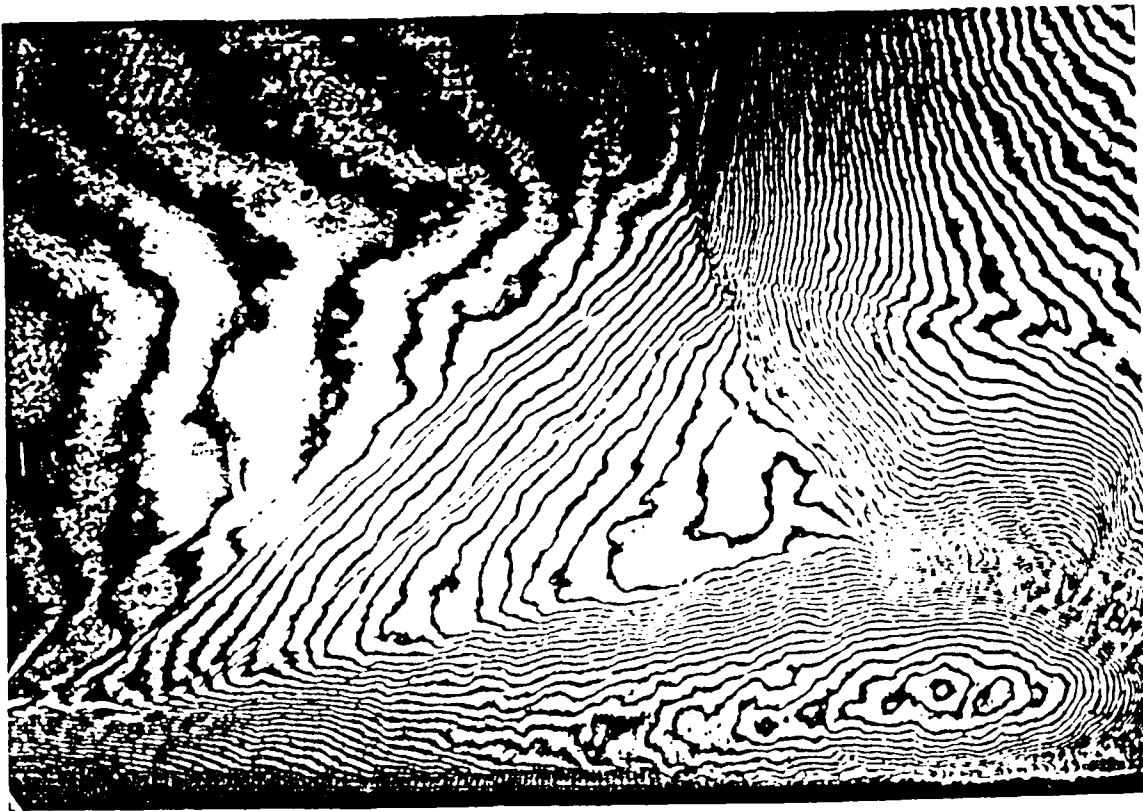


Figure 6 Scaling Of Reduced Upstream Influence and Shock Angles



Setup Diagram for Conical Holographic Interferometry of Swept Shock/- Boundary Layer Interactions

Figure 7



Mach 2.97, $\alpha = 20^\circ$

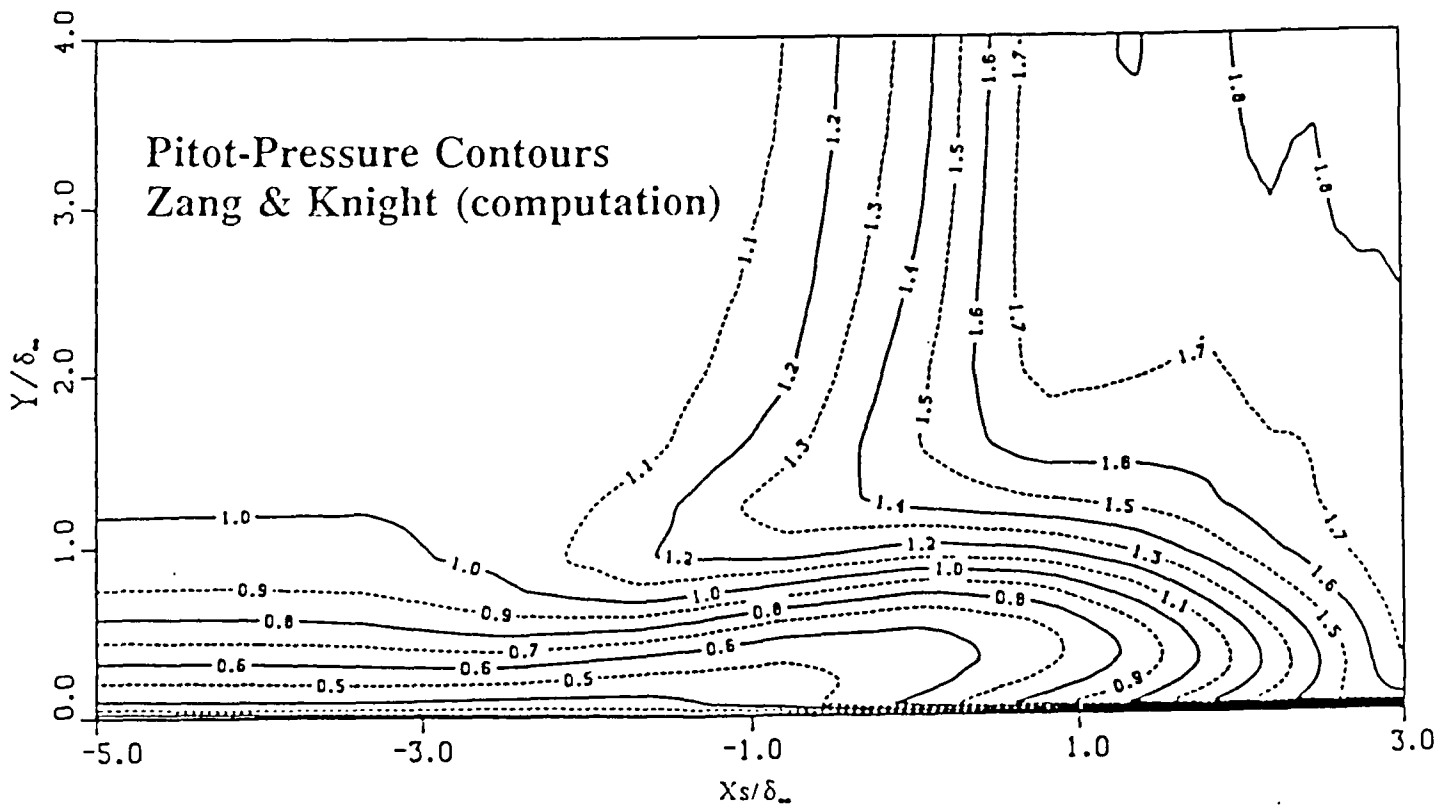


Figure 8b Comparison Of Holographic Interferogram and Computed Pitot Contours Of Zang and Knight

Interaction Strength Correlation

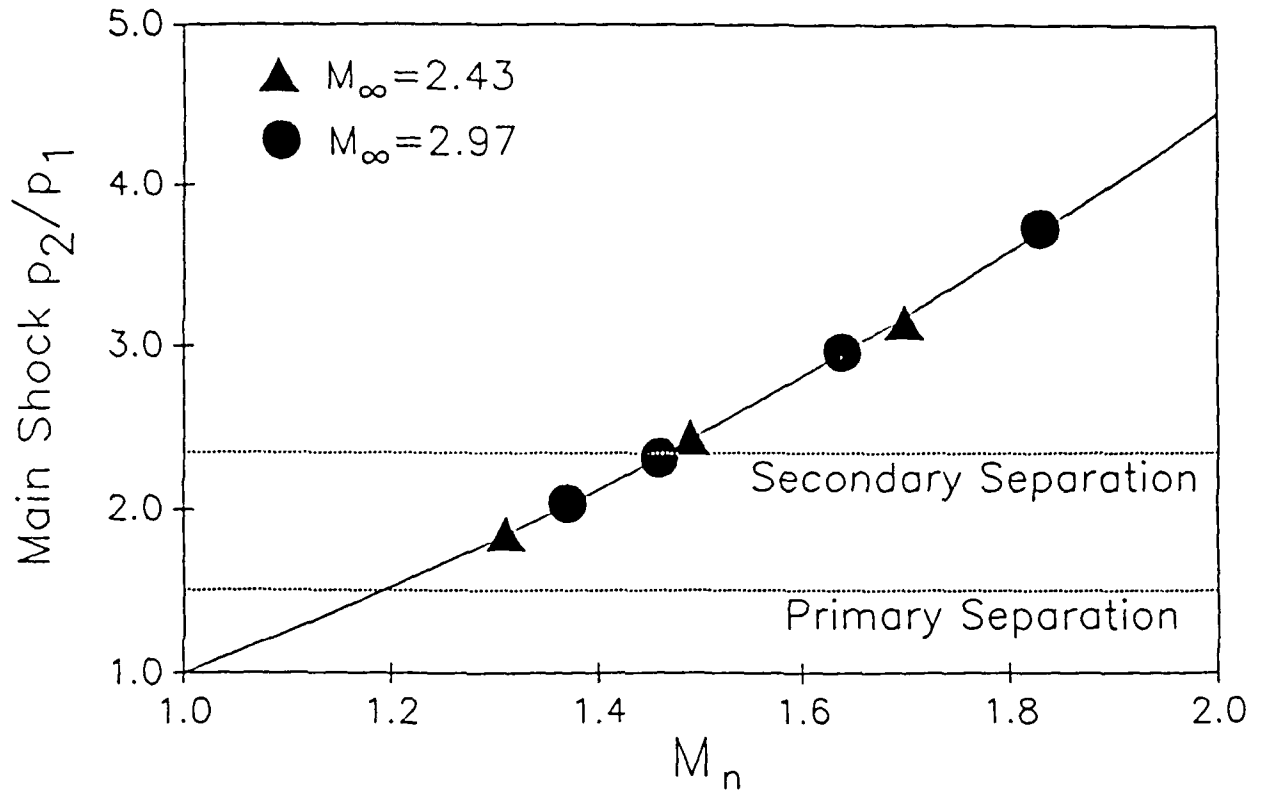
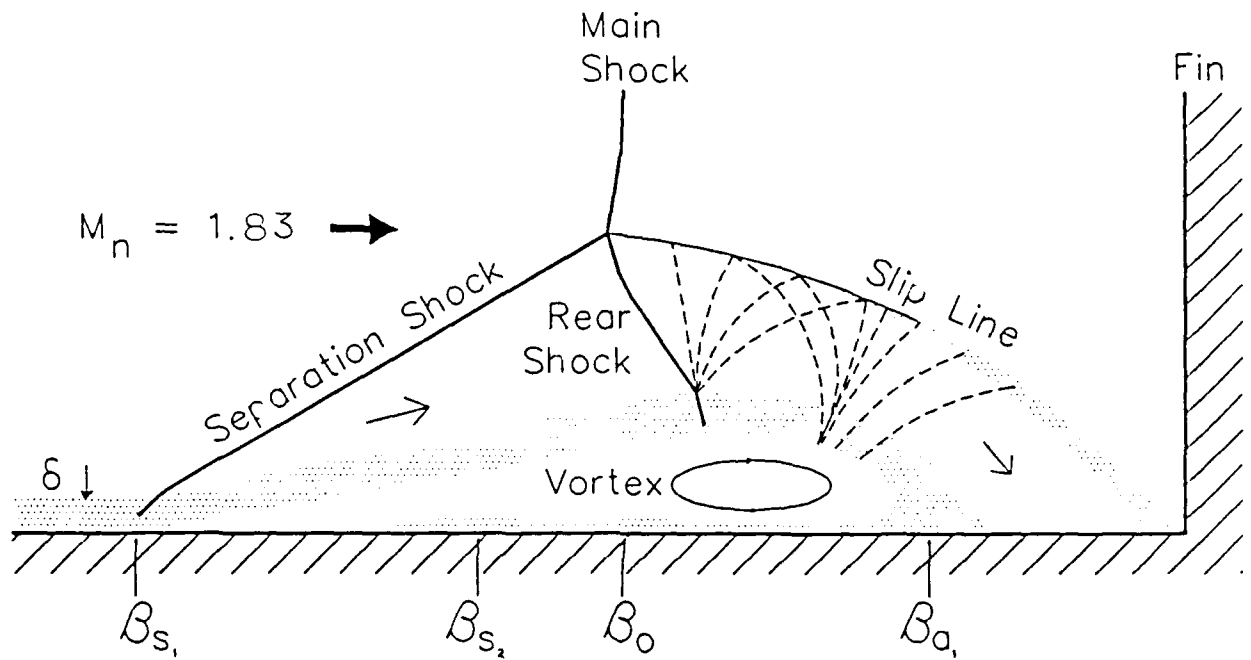


Figure 9



Present Model of Interaction Flowfield Structure

(Based on Mach 3, $\alpha = 20^\circ$)

Figure 10

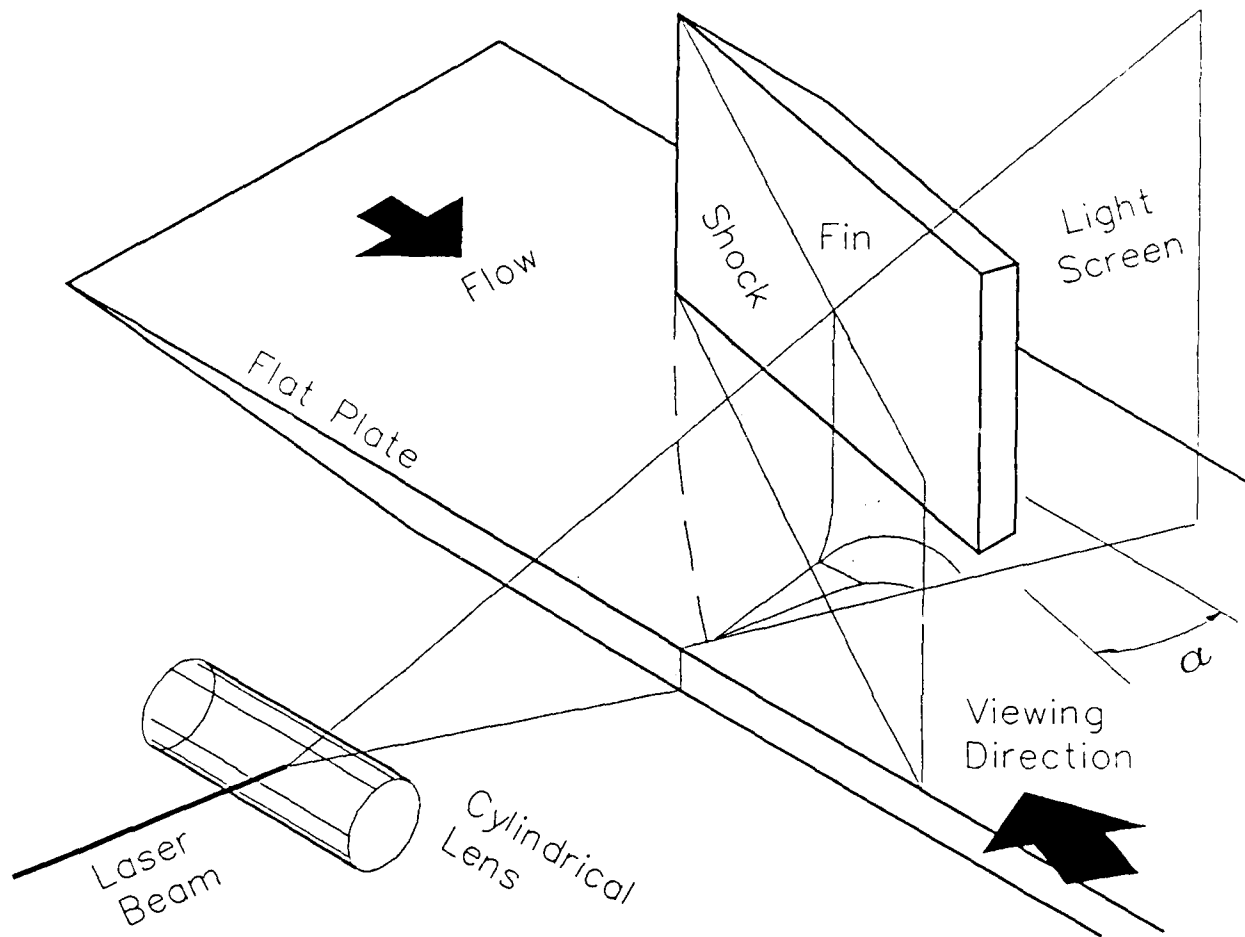


Figure 11 Diagram Of LLS Experimental Setup

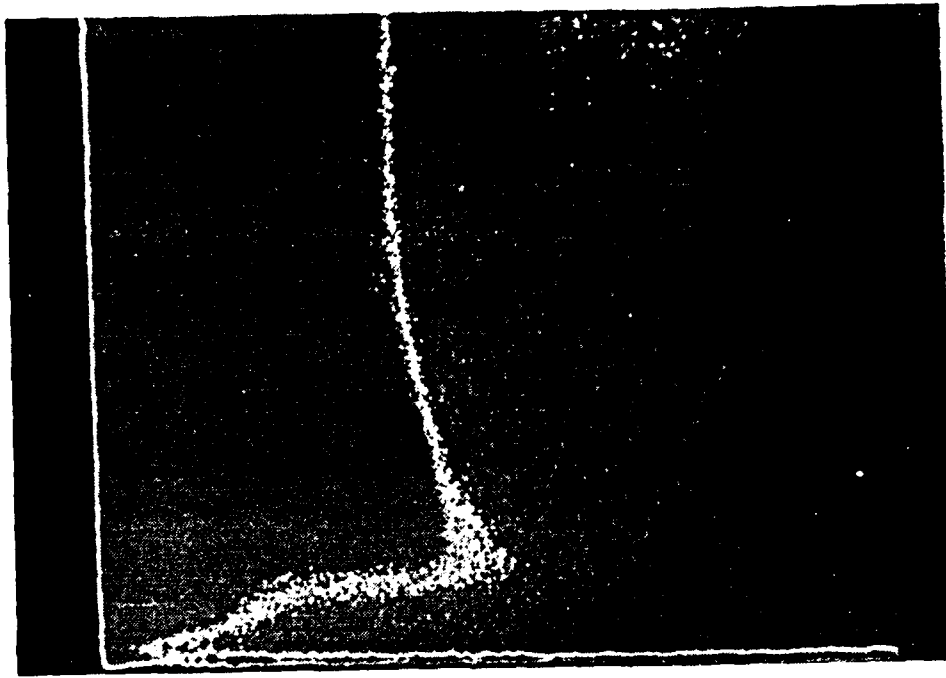


Figure 12 LLS Image Of Fin Interaction At Mach 2.47, $\alpha = 10^\circ$

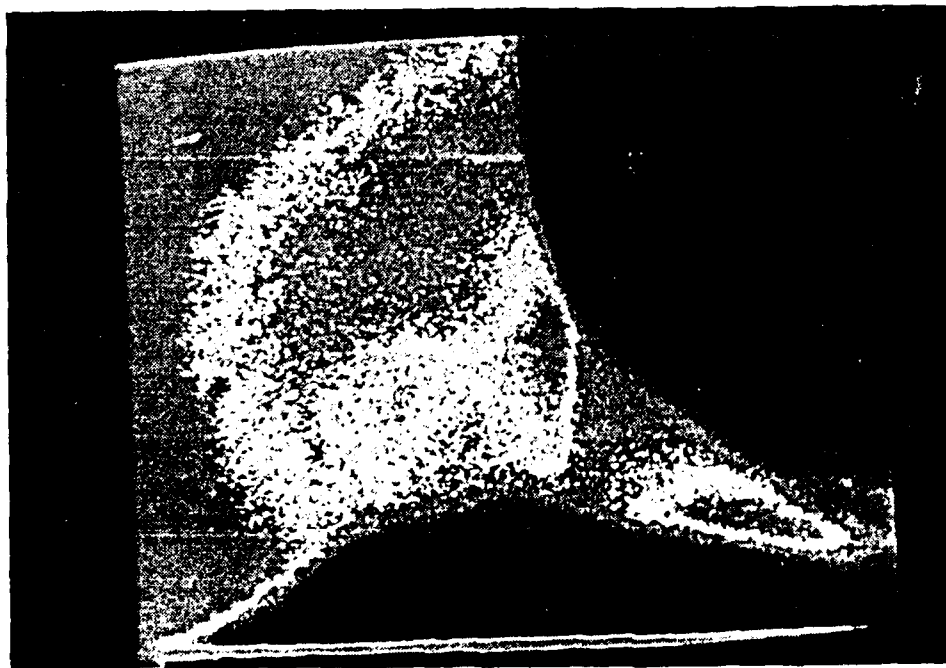


Figure 13 LLS Image Of Fin Interaction At Mach 3.44, $\alpha = 10^\circ$

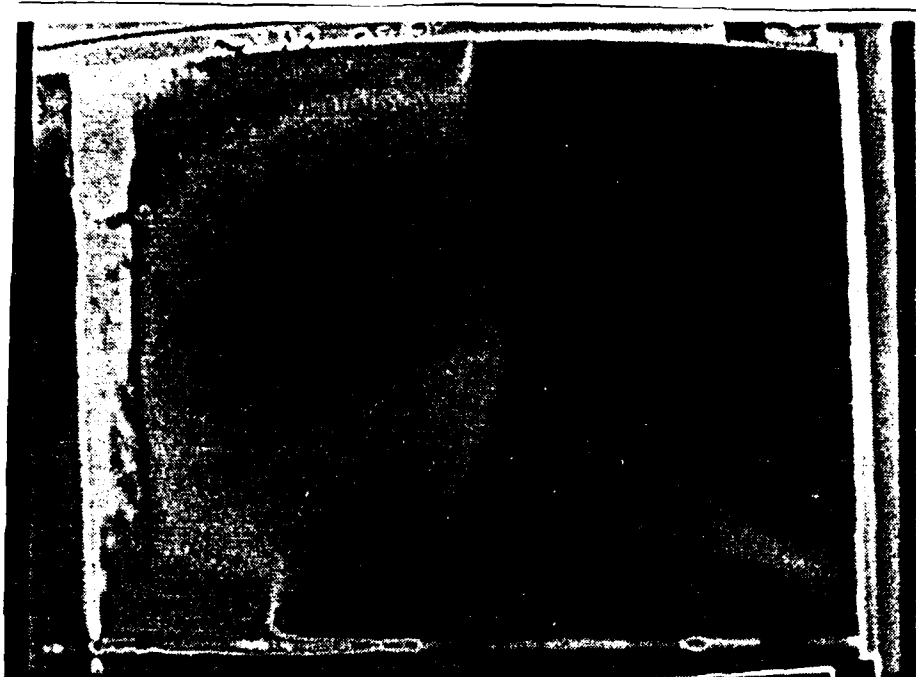


Figure 14 LLS Image Of Fin Interaction At Mach 3.44, $\alpha = 15^\circ$

PENNSTATE



Gas Dynamics Lab

Contour Shadowgram of Fin
Interaction, Mach 3, $\alpha = 20^\circ$

Flow →

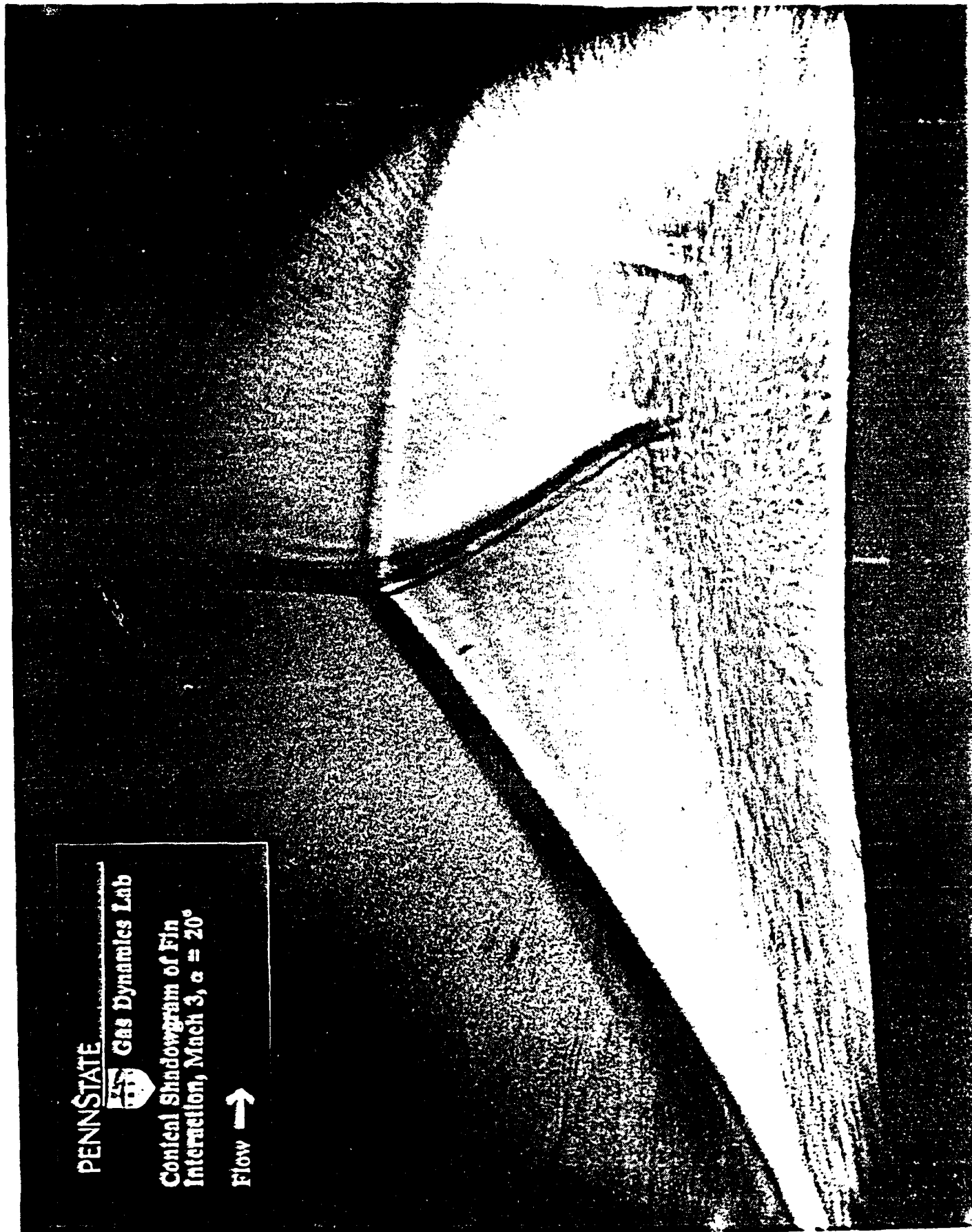


Figure 15

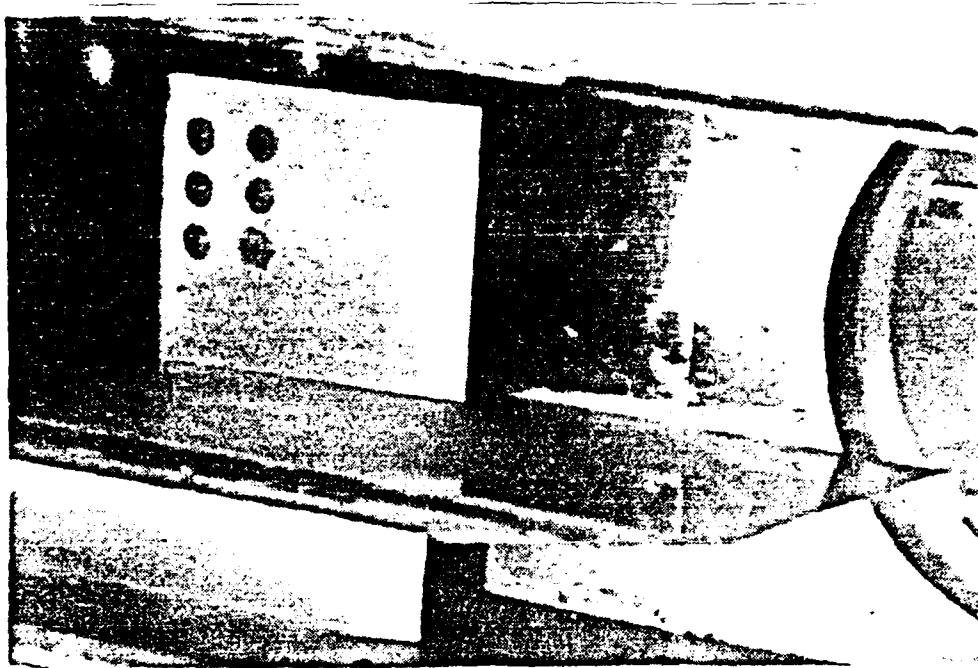


Figure 17 Photo Of Fix. Plate Installation

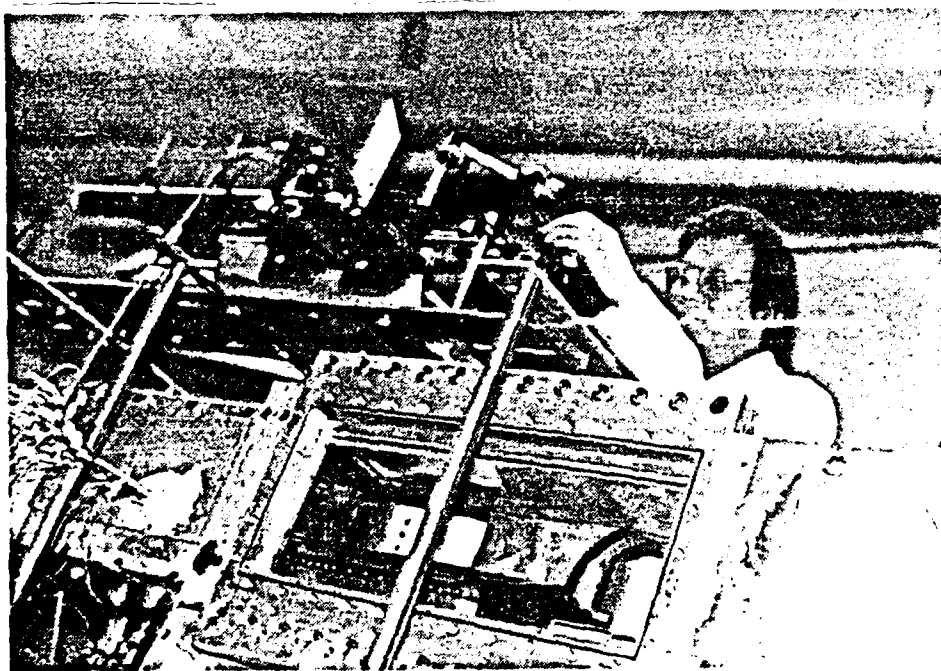


Figure 18 LISI Instrument Installed Above Test Section

MACH 3, 10° FIN C_f DISTRIBUTION

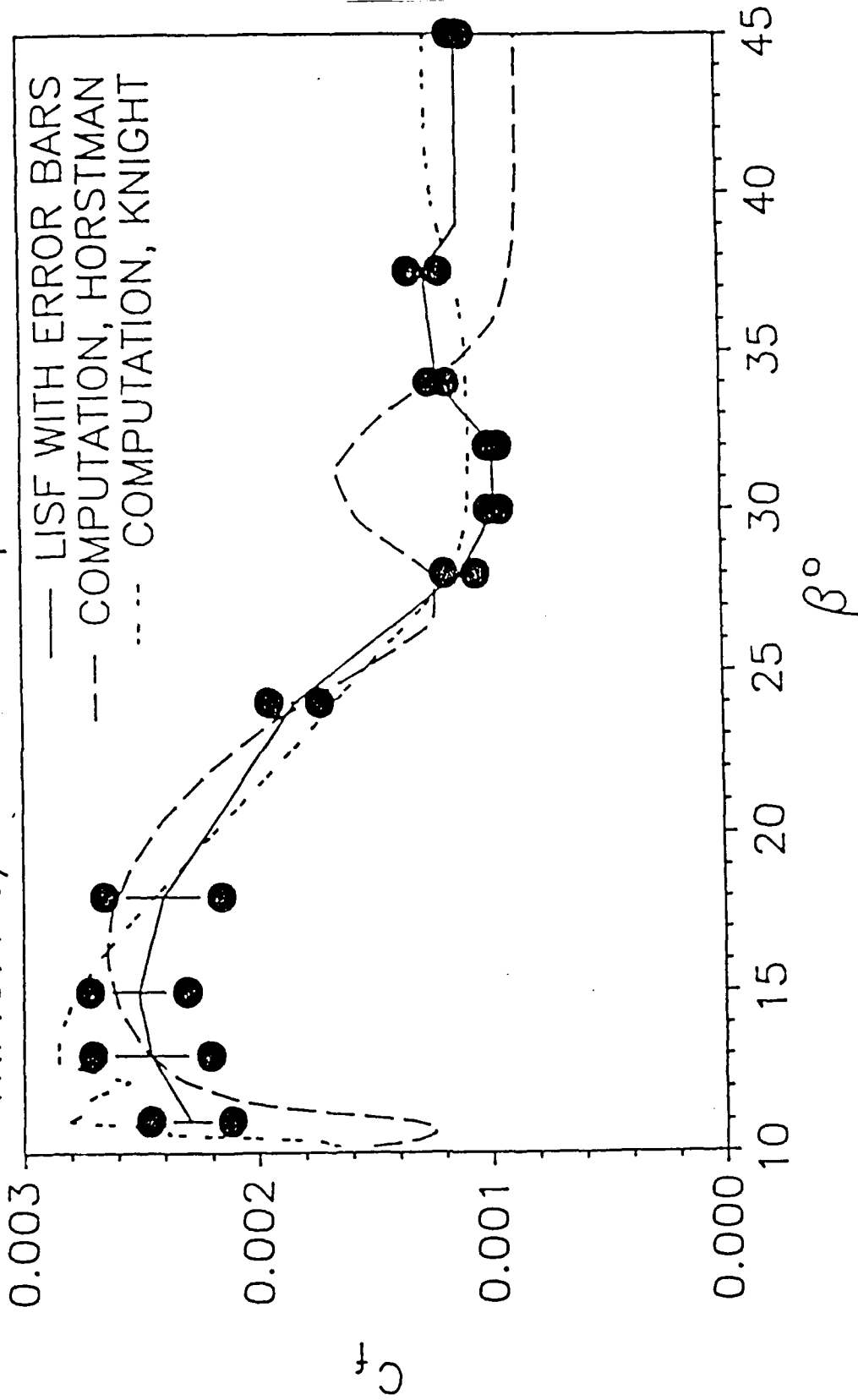


Figure 19

Mach 3, 16° Fin Skin Friction Distribution

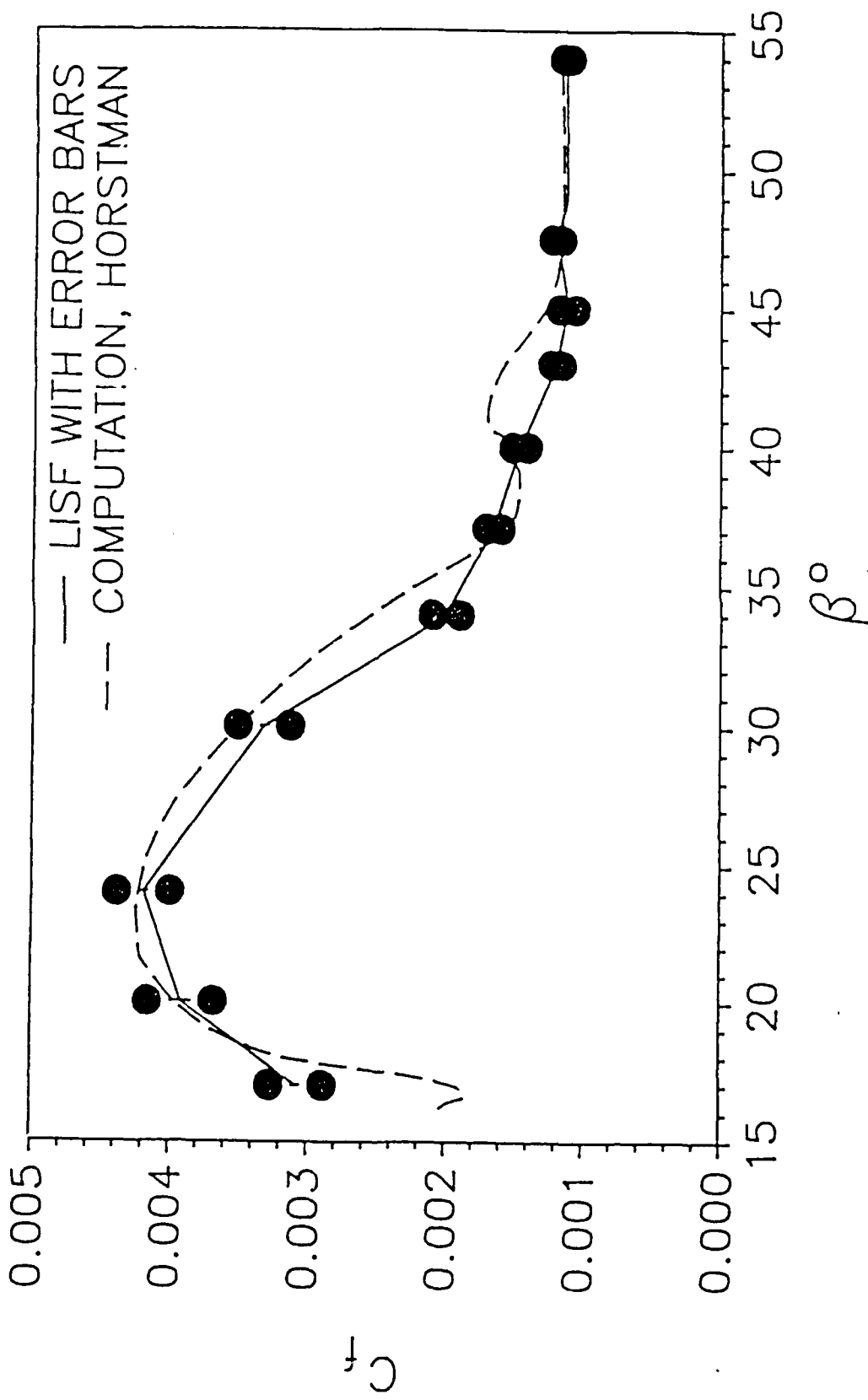


Figure 20

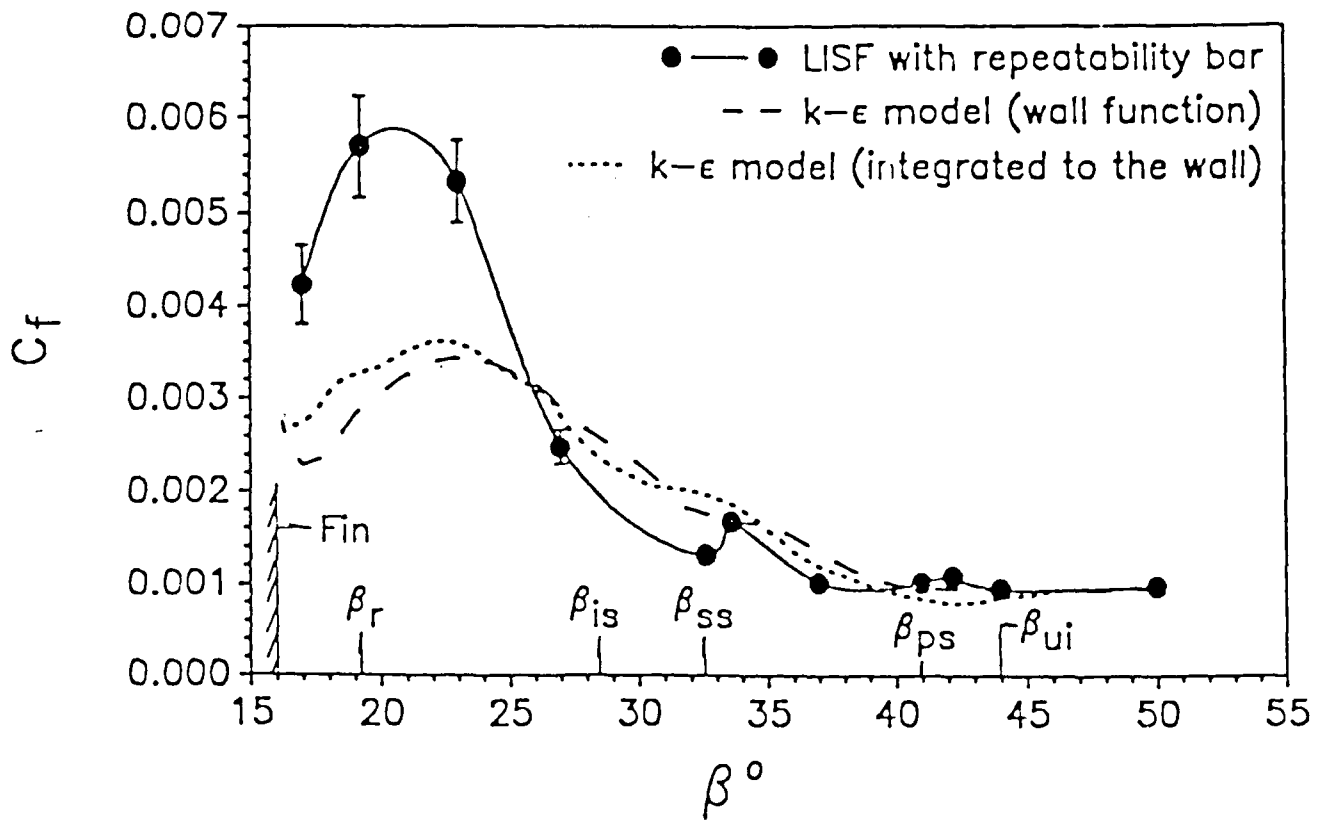


Figure 21 - c_f Distribution for Mach 4, $\alpha = 16^\circ$ with CFD comparison.

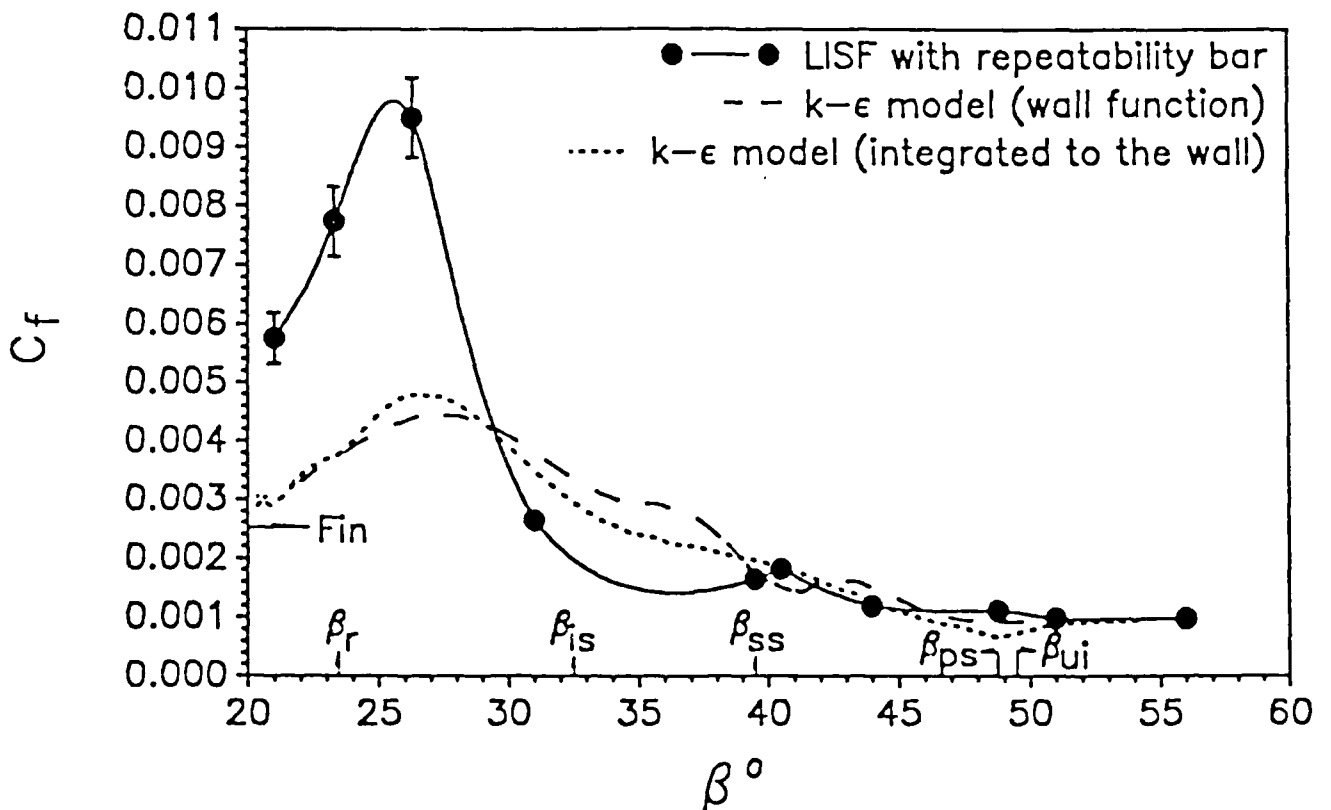


Figure 22 c_f Distribution for Mach 4, $\alpha = 20^\circ$ with CFD comparison.

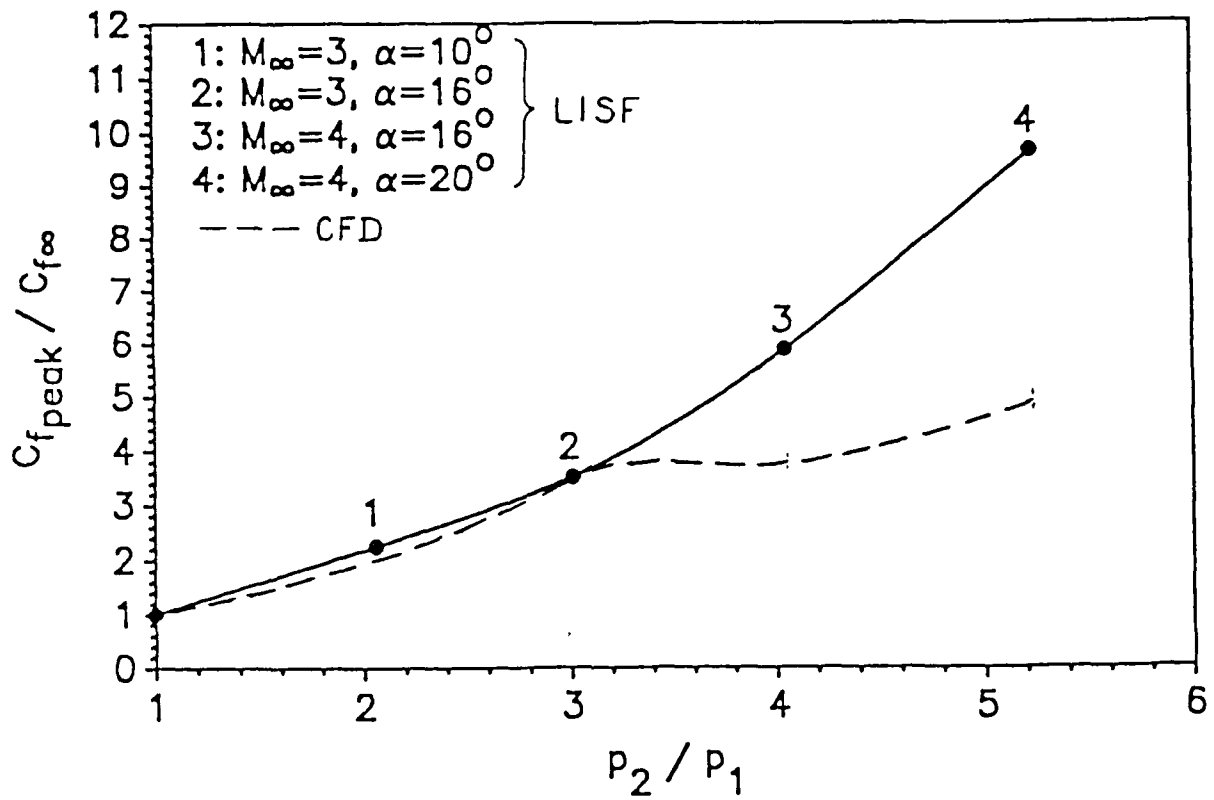


Figure 23 Variation of $c_{f,peak}/c_{f_\infty}$ with Interaction Strength.